C. elegans establishes germline versus soma by balancing inherited histone methylation

Brandon S. Carpenter[1], Teresa W. Lee[1], Caroline F. Plott[2], Jovan S. Brockett[3], Dexter A. Myrick[1], David J. Katz[1*]

[1]Department of Cell Biology, Emory University School of Medicine, Atlanta GA 30322, USA.

[2]Johns Hopkins University School of Medicine, Baltimore MD 21205, USA.

[3]Department of Biology, Oglethorpe University, Atlanta GA 30319, USA.

*corresponding author:
David J. Katz
Associate Professor
Department of Cell Biology
Room 443, Whitehead Biomedical Research Building
Emory University School of Medicine
Atlanta, GA 30322, USA
Phone: (404) 727-3403
djkatz@emory.edu

ABSTRACT

Embryos undergo extensive reprogramming at fertilization to prevent the inappropriate inheritance of histone methylation. In *C. elegans,* this reprogramming is mediated by the H3K4me2 demethylase, SPR-5, and the H3K9 methyltransferase, MET-2. In contrast to this reprogramming, the H3K36 methyltransferase, MES-4, maintains H3K36me2/3 at germline genes between generations to help re-establish the germline. To determine whether the MES-4 germline inheritance system antagonizes *spr-5; met-2* reprogramming, we examined the interaction between these two systems. We find that the developmental delay of *spr-5; met-2* mutant progeny is associated with ectopic H3K36me2/3 and the ectopic expression of MES-4 targeted germline genes in somatic tissues. Furthermore, the developmental delay is dependent upon MES-4 and the H3K4 methyltransferase, SET-2. We propose that the MES-4 inheritance system prevents critical germline genes from being repressed by maternal *spr-5; met-2* reprogramming. Thus, the balance of inherited histone modifications is necessary to distinguish germline versus soma and prevent developmental delay.

INTRODUCTION

In multicellular organisms, developmental cell fate decisions are established by tightly controlled spatial and temporal gene expression. This pattern of gene expression can be regulated by heritable modifications on the N-terminal tails of histone proteins (Jambhekar et al., 2019). For example, methylation of either lysine 4 or 36 on histone 3, (H3K4me and H3K36me) is generally associated with active transcription, whereas methylation of lysine 9 on the same histone (H3K9me) is commonly associated with transcriptional repression. These modifications are dynamically regulated by the specific

24 and tightly controlled activity of histone modifying enzymes. For instance, mono- and di-
25 methylation of lysine 4 on histone H3 (H3K4me1/2) are removed by the demethylase
26 LSD1/KDM1A (Y. Shi et al., 2004; Y.-J. Shi et al., 2005). In the nematode *C. elegans*,
27 populations of mutants lacking the LSD1 ortholog, SPR-5, become increasingly sterile over
28 ~30 generations (Katz et al., 2009). Failure to erase H3K4me2 at fertilization between
29 generations in *spr-5* mutants correlates with an accumulation of H3K4me2 and
30 spermatogenesis gene expression across 30 generations, which leads to increasing sterility
31 (Katz et al., 2009). These data demonstrate that H3K4me2 can function as an epigenetic
32 transcriptional memory. More recently, we demonstrated that SPR-5 synergizes with the
33 H3K9me2 methyltransferase, MET-2, to regulate maternal epigenetic reprogramming (Kerr
34 et al., 2014). Progeny of mutants lacking both SPR-5 and MET-2 suffer from developmental
35 delay and become completely sterile in a single generation (Kerr et al., 2014). These
36 phenotypes are associated with synergistic increases in both H3K4me2 and candidate
37 germline gene expression in somatic tissues (Kerr et al., 2014). Together this work
38 supports a model in which SPR-5 and MET-2 are maternally deposited into the oocyte,
39 where they reprogram histone methylation to prevent inherited defects.
40 Following fertilization, the *C. elegans* embryo separates germline versus somatic
41 lineages progressively through a series of asymmetric divisions (Strome, 2005). To
42 accomplish this, transcription factors coordinate with multiple histone modifications. For
43 example, maternal deposition of PIE-1, a germline specific protein that asymmetrically
44 segregates into germline blastomeres (P lineage cells), maintains the fate of germ cells by
45 inhibiting POL-II elongation and preventing the ectopic expression of somatic genes
46 (Batchelder et al., 1999; Mello et al., 1992; Seydoux et al., 1996). In the absence of

47 transcription in the germline, the maternally provided H3K36me2/3 methyltransferase,
48 MES-4, binds to a subset of germline genes that were previously expressed in the parental
49 germline (Furuhashi et al., 2010; Rechtsteiner et al., 2010). These germline genes are
50 recognized by MES-4 via H3K36me2/3 that was added in the parental germline by the
51 transcription-coupled H3K36me2/3 methyltransferase, MET-1 (Kreher et al., 2018). MES-4
52 maintains H3K36me2/3 at these genes in the early embryo in a transcriptionally
53 independent manner. Without maternally deposited MES-4, the germline cannot properly
54 proliferate and animals are sterile (Capowski et al., 1991; Garvin et al., 1998). For the
55 remainder of this study, we will refer to these MES-4 targeted genes as MES-4 germline
56 genes, and the process through which the MES-4 germline inheritance system maintains
57 these genes for re-activation in the offspring as bookmarking.
58 MES-4 bookmarking is antagonized in somatic tissues by transcriptional repressors
59 and chromatin remodelers. For example, loss of the transcriptional repressors LIN-15B and
60 LIN-35 at high temperatures leads to larval arrest (Petrella et al., 2011). This larval arrest
61 can be suppressed by removing the MES-4 germline inheritance system (Petrella et al.,
62 2011). Removing the MES-4 inheritance system also suppresses the somatic expression of
63 germline genes in *lin-35* mutants (Wang et al., 2005). Similar to LIN-15B and LIN-35, loss of
64 the chromatin remodelers MEP-1 and LET-418 causes somatic expression of germline
65 genes and larval arrest (Unhavaithaya et al., 2002). This somatic expression of germline
66 genes and larval arrest is also dependent upon the MES-4 germline inheritance system
67 (Unhavaithaya et al., 2002). Together, these findings demonstrate that transcriptional
68 repressors and the chromatin remodelers function in somatic tissues to antagonize H3K36
69 bookmarking by MES-4.

70 Recently, the repressive histone modification H3K9me2 has also been implicated in
71 the somatic repression of germline genes (Rechtsteiner et al., 2019). Some germline genes
72 have H3K9me2 enrichment at their promoters in somatic tissues (Rechtsteiner et al.,
73 2019). Loss of LIN-15B reduces this enrichment of H3K9me2 leading to the ectopic
74 accumulation of H3K36me3 at gene bodies in somatic tissues (Rechtsteiner et al., 2019).
75 This raises the possibility that LIN-15B may antagonize the MES-4 germline inheritance in
76 part through the repressive histone modification H3K9me2.
77 Despite the extensive knowledge of the systems that somatically antagonize the
78 MES-4 germline inheritance system, it remains unclear why germline genes are
79 bookmarked by H3K36 in the embryo. To address this major gap, we examined somatic
80 development in progeny deficient in SPR-5 and MET-2 maternal reprogramming. Our
81 previous work suggests that maternal *spr-5; met-2* reprogramming prevents the
82 transgenerational inheritance of H3K4me2 by erasing this mark and coupling it to the
83 acquisition of H3K9me2 between generations (Kerr et al., 2014). Here we show that
84 H3K36me3 ectopically accumulates at MES-4 germline genes in the somatic tissues of *spr-*
85 *5; met-2* double mutant progeny (hereafter referred to as *spr-5; met-2* progeny), and this
86 accumulation correlates with the ectopic expression of these genes. In addition, we find
87 that both the developmental delay and the ectopic expression of germline genes is rescued
88 by knocking down MES-4 activity. These data provide comprehensive evidence that the
89 ectopic expression of MES-4 targeted germline genes in somatic tissues causes
90 developmental delay. In addition, we demonstrate that the severe developmental delay of
91 *spr-5; met-2* progeny is rescued by the loss of the H3K4 methyltransferase SET-2. This
92 finding suggests that the ectopic maintenance of the MES-4 germline inheritance system in

93 *spr-5; met-2* progeny is driven by the inheritance of H3K4 methylation. Finally, by
94 demonstrating that loss of maternal *spr-5; met-2* reprogramming unbalances the MES-4
95 germline inheritance system, our data suggest that H3K36 methylation bookmarking
96 functions to antagonize *spr-5; met-2* maternal reprogramming. Thus, we propose that *C.*
97 *elegans* balances three different histone modifications to distinguish between the
98 competing fates of soma and germline.
99

100 **RESULTS**

101 **Loss of *spr-5* and *met-2* causes a severe developmental delay**

102 Previous observations from our lab indicated that progeny from *spr-5; met-2*
103 mutants may develop abnormally (Kerr et al., 2014). To further characterize this
104 phenotype, we synchronized embryos laid by N2, *spr-5*, *met-2*, and *spr-5; met-2* mutant
105 hermaphrodites and monitored their development from hatching to adults. By 72 hours,
106 all N2 progeny (469/469), most of the *spr-5* progeny (363/385), and many of *met-2*
107 progeny (386/450) were fertile adults (Figure 1A, B, C, and E, Figure 1-figure supplement
108 1A-C). In contrast, *spr-5; met-2* progeny displayed a severe developmental delay, with none
109 of the progeny (0/463) reaching adulthood by 72 hours (Figure 1D, E; and Figure 1-figure
110 supplement 1D). The majority of *spr-5; met-2* progeny (371/463) resembled L2 larvae at
111 72 hours, while a smaller percentage of the population developed to later larval stages
112 (42/463) (supplementary file 1). By seven days post synchronized lay, a small number of
113 *spr-5; met-2* progeny (35/876) developed into adults and the majority (31/35) of these
114 adults displayed protruding vulva (Pvl) (Figure 1-figure supplement 1E-G). All 35 of the
115 *spr-5; met-2* mutant progeny that developed to adulthood were sterile.

116

117 **MES-4 germline genes are ectopically expressed in *spr-5; met-2* mutant soma**

118 Previously we showed that H3K4me2 is synergistically increased in *spr-5; met-2*
119 progeny compared to *spr-5* and *met-2* single mutant progeny, and that this increase in
120 H3K4me2 correlates with a synergistic increase in candidate germline gene expression in
121 somatic tissues (Kerr et al., 2014). To test the extent to which germline genes are
122 ectopically expressed in somatic tissues, we examined somatic expression genome-wide.
123 To do this, we performed RNA-seq on *spr-5; met-2* L1 progeny compared to N2 (wild-type)
124 L1 progeny. We chose to perform this analysis on L1 larvae because this stage immediately
125 precedes the L2 larval delay that we observe in *spr-5; met-2* progeny (see Figure 1A, D). In
126 addition, L1 larvae are composed of 550 somatic cells and two germ cells. Therefore, L1
127 larvae are primarily composed of somatic tissue. As a control, we also performed RNA-seq
128 on L1 progeny from *spr-5* and *met-2* single mutants that were isolated from early
129 generation animals, within the first five generations. These generations are well before the
130 onset of sterility that we previously reported (Katz et al., 2009; Kerr et al., 2014).

131 We identified 778 differentially expressed transcripts in *spr-5; met-2* progeny
132 compared to N2 (Figure 2-supplement figure 1A-B, Figure 2-supplement figure 2C, F, and
133 supplementary file 2), many of which also overlap with genes differentially expressed in
134 *spr-5* (159/413) and *met-2* single mutants (113/343) compared to N2 (Figure 2-
135 supplement figure 1A-B, Figure 2-supplement figure 2A, B, D, E, and supplementary file 2).
136 Gene Set Enrichment Analysis (GSEA) did not identify any categories of genes
137 misexpressed in the *spr-5* or *met-2* single mutants. However, GSEA revealed that genes
138 differentially expressed in *spr-5; met-2* progeny were significantly enriched (based on

139 Combined Score, (Chen et al., 2013)) for biological processes and cellular components
140 characteristic of the germline; including meiosis, P-granules and negative regulation of the
141 cell cycle (Figure 2-supplement figure 1C-D). Many of the genes involved in these processes
142 are expressed in the germline of the parental generation, bound by the H3K36
143 methyltransferase MES-4 in the early embryo, and marked by H3K36me2/3, independent
144 of POL-II (Rechtsteiner et al., 2010). As a result, we were interested in the potential overlap
145 with MES-4 targeted genes (referred to as MES-4 germline genes).

146 Rechtsteiner and colleagues identified approximately 200 MES-4 germline genes
147 (Rechtsteiner et al., 2010). We reasoned that the absence of SPR-5 and MET-2
148 reprogramming may cause germline genes to be aberrantly targeted by MES-4 in the soma,
149 leading to ectopic expression. To investigate this possibility, we examined the overlap
150 between differentially expressed genes in *spr-5; met-2* L1 progeny and MES-4 germline
151 genes. Out of 196 MES-4 germline genes, 34 overlapped with genes up-regulated in *spr-5;*
152 *met-2* progeny compared to N2 (Figure 2A, hypergeometric test, p-value < 6.44e-20), while
153 zero overlapped with genes down-regulated in *spr-5; met-2* progeny compared to N2
154 (Figure 2B). In addition, when we compared the log2 fold change (FC) in expression of all of
155 the MES-4 germline genes in *spr-5*, *met-2*, and *spr-5; met-2* mutant progeny compared to
156 N2, we observed that 108 of the MES-4 germline genes were synergistically increased in
157 *spr-5; met-2* progeny compared to single mutant progeny (Figure 2C and supplementary
158 file 3).

159 During this initial RNA-seq analysis we had to genotype every *spr-5; met-2* L1
160 because the balancer chromosome that was available did not completely balance *spr-5*. As a
161 result, the RNA-seq was performed using a low-input sequencing technique (see methods).

162 However, during the course of the experiments, a new balancer became available that
163 completely balances *spr-5*. This enabled us to repeat the *spr-5; met-2* RNA-seq experiments
164 using standard amounts of RNA. In the repeat *spr-5; met-2* RNA-seq experiment, we
165 identified significantly more differentially expressed genes compared to N2 (4223 vs. 778
166 in the initial low-input analysis). However, despite the larger number of differentially
167 expressed genes, MES-4 germline genes remained similarly enriched. Out of 196 MES-4
168 germline genes, 112 overlapped with genes up-regulated in *spr-5; met-2* progeny compared
169 to N2 (Figure 2-supplemental figure 3A, hypergeometric test, P-value < 1.20e-54, and
170 supplementary file 2), while only two overlapped with genes down-regulated in *spr-5; met-*
171 *2* progeny compared to N2 (Figure 2-supplemental figure 3B). We also compared the
172 log2FC in expression of all of the MES-4 germline genes in *spr-5; met-2* mutant progeny
173 compared to N2. This analysis revealed that the MES-4 germline genes were similarly
174 overexpressed in *spr-5; met-2* progeny compared to N2 (Figure 2D and supplementary file
175 3). Interestingly, while MES-4 germline genes were enriched in both *spr-5; met*-2 RNA-seq
176 experiments, there were some differences in the specific MES-4 germline genes that were
177 overexpressed, and the extent to which they were overexpressed (Figure 2-supplemental
178 figure 3C and supplementary file 3).
179

180 **smFISH confirmation of MES-4 germline gene expression in *spr-5; met-2* mutant**
181 **soma**

182 To confirm that MES-4 germline genes are somatically expressed in *spr-5; met-2* L1
183 progeny, we performed single molecule fluorescent *in situ* hybridization (smFISH) on two
184 MES-4 germline targets, *htp-1* and *cpb-1* (Figure 3). Both of these genes were amongst the

185 genes that were ectopically expressed in *spr-5; met-2* L1 progeny compared to N2 L1
186 progeny. In N2 L1 larvae, *htp-1* (Figure 3A-C, insets) and *cpb-1* (Figure 3G-I, insets) were
187 restricted to the two primordial germ cells, Z2 and Z3, which go on to form the entire adult
188 germline. This confirms that these transcripts are confined to the germline as expected. In
189 contrast, in *spr-5; met-2* progeny *htp-1* was ectopically expressed throughout the soma
190 (Figure 3D-F). This expression pattern is similar to what we observed with the
191 ubiquitously expressed subunit of RNA polymerase II, *ama-1* (Figure 3-supplement figure
192 1A-L), which was unchanged in our RNA-seq analysis. *cpb-1* was also ectopically expressed
193 in *spr-5; met-2* progeny, though the ectopic expression was not as ubiquitous as *htp-1*
194 (Figure 3J, L).
195
196 **MES-4 germline genes maintain ectopic H3K36me3 in *spr-5; met-2* mutants**
197 To test whether MES-4 germline genes that are ectopically expressed in the soma of
198 *spr-5; met-2* progeny also ectopically maintain H3K36me3, we performed H3K36me3 ChIP-
199 seq. MES-4 germline genes have low levels of H3K36me3 in N2 L1 progeny. However,
200 compared to N2 L1 progeny, *spr-5; met-2* L1 progeny displayed increased enrichment for
201 H3K36me3 across gene bodies at MES-4 germline genes (Figure 4A, B; Figure 4-
202 supplement figure 1A, B, Q-R). For example, the MES-4 germline genes *cpb-1*, *T05B9.1,*
203 *Y18D10A.11*, and *fbxa-101,* that are ectopically expressed in our RNA-seq analysis, showed
204 increased levels of H3K36me3 in *spr-5; met-2* progeny (Figure 4J-M; Figure 4-supplement
205 figure 1J-M) compared to N2 progeny (Figure 4C-F; Figure 4-supplement figure 1C-F). As a
206 control, we examined H3K36me3 enrichment at genes that are not affected in *spr-5; met-2*
207 progeny. These control genes include: *ceh-13*, a gene enriched in hypodermal and ventral

208 nerve chord in L1 progeny (Figure 4G, N; Figure 4-supplement figure 1G, N), *ama-1*, a
209 subunit of RNA polymerase II that is expressed ubiquitously (Figure 4H, O; Figure 4-
210 supplement figure 1H, O), and *act-1*, a ubiquitously expressed actin related protein (Figure
211 4I, P; Figure 4-supplement figure 1I, P). Each of these control genes displayed similar
212 H3K36me3 enrichment in both *spr-5; met-2* and N2 L1 progeny (compare Figure 4N-P and
213 Figure 4-supplement figure 1N-P to Figure 4G-I and Figure 4-supplement figure 1G-I,
214 respectively).
215
216 **MES-4 germline genes display H3K9me2 at their promoter peaks**
217 Recent work discovered that some germline specific genes contain H3K9me2 peaks
218 at their promoters in N2 L1 progeny (Rechtsteiner et al., 2019). This finding implicates
219 H3K9me2 enrichment at promoters of germline genes as being a critical component for
220 repressing germline genes in somatic tissues. If SPR-5 and MET-2 are functioning to
221 prevent MES-4 germline genes from being ectopically expressed in somatic tissues, we
222 would expect MES-4 germline genes that are ectopically expressed in the somatic tissues of
223 *spr-5; met-2* progeny to normally continue to be targeted by H3K9 methylation in these
224 tissues. To examine this possibility, we re-analyzed L1 stage H3K9me2 Chip-seq data from
225 Rechsteiner et al. 2019 (Rechtsteiner et al., 2019). This re-analysis showed that many of the
226 MES-4 germline genes were enriched for H3K9me2 at their promoters (Figure 4-
227 supplement figure 2A), including the majority of MES-4 germline genes that were
228 ectopically expressed in the soma of *spr-5; met-2* progeny (Figure 4-supplement figure 2B).
229 For example, the MES-4 germline genes *cpb-1*, *T05B9.1*, *Y18D10A.11*, and *fbxa-101*, that
230 were misexpressed somatically and accumulated ectopic H3K36me3 in the somatic tissues

231 of *spr-5; met-2* progeny, had H3K9me2 peaks at their promoters (Figure 4-supplement
232 figure 2C-F). In contrast, our control genes *ceh-13*, *ama-1*, and *act-1*, that were not
233 misexpressed, were also not enriched for H3K9me2 at their promoters (Figure 4-
234 supplement figure 2G-I).
235
236 **Knocking down MES-4 rescues ectopic expression of germline genes in *spr-5; met-2***
237 **mutant soma**
238 To test whether the ectopic expression of MES-4 germline genes in *spr-5; met-2*
239 progeny is dependent on the ectopic H3K36me3, we examined whether the expression of
240 these genes was dependent upon MES-4. We performed quantitative real-time PCR (qRT-
241 PCR) on L1 progeny from *spr-5; met-2* hermaphrodites fed control (L4440) RNAi versus
242 *mes-4* RNAi (Figure 5). For this analysis, we selected candidate MES-4 germline genes that
243 were ectopically expressed and displayed an ectopic H3K36me3 peak in *spr-5; met-2* L1
244 progeny compared to N2 L1 progeny. Consistent with our RNA-seq analysis, all nine of the
245 candidate MES-4 germline genes that we examined were ectopically expressed >2 fold in
246 *spr-5; met-2* L1 progeny compared to control (Figure 5). Strikingly, the ectopic expression
247 of the nine MES-4 candidate germline genes was dependent upon MES-4. Nine out of nine
248 of these genes were significantly decreased in L1 progeny from *spr-5; met-2*
249 hermaphrodites treated with *mes-4* RNAi (Figure 5; unpaired t-test, p-value < 0.001), and
250 all but one (*T05B9.1*) were reduced to levels that were similar to N2 L1 progeny.
251
252 **Knocking down MES-4 rescues developmental delay in *spr-5; met-2* progeny**

253 To test whether the developmental delay phenotype that we observe in *spr-5; met-2*
254 progeny is also dependent on the ectopic expression of MES-4 germline genes, we fed *spr-5;*
255 *met-2* hermaphrodites *mes-4* RNAi and monitored their progeny for 72 hours after a
256 synchronized lay. If the developmental delay is dependent upon the ectopic expression of
257 MES-4 germline genes, it should be suppressed when this ectopic expression is eliminated
258 via *mes-4* RNAi. By 72 hours, all of the N2 control progeny from hermaphrodites fed either
259 L4440 control (1089/1089) or *mes-4* (1102/1102) RNAi were adults (Figure 6A, B, I). Also,
260 consistent with our previous observations, all but one of the *spr-5; met-2* mutant progeny
261 (729/730) from hermaphrodites fed control RNAi remained in the L2-L3 larval stages
262 (Figure 6E, I). In contrast, most of *spr-5; met-2* progeny (569/618) from hermaphrodites
263 fed *mes-4* RNAi developed to adults (Figure 6F, I, unpaired t-test, $p<0.0001$). Though as
264 expected, these animals remained sterile due to the *mes-4* RNAi preventing any germline
265 formation.
266 MET-1 mediates transcription-coupled H3K36me3 in the adult germline and in later
267 stage transcriptionally active embryos (Furuhashi et al., 2010; Kreher et al., 2018;
268 Rechtsteiner et al., 2010). If the ectopic somatic expression of MES-4 germline genes is
269 caused by the transcription independent maintenance of H3K36me3 via MES-4, we would
270 expect the developmental delay to be independent of MET-1. To determine whether the
271 developmental delay phenotype in *spr-5; met-2* progeny is dependent on MET-1, we
272 monitored the development of progeny from *spr-5; met-2* hermaphrodites fed *met-1* RNAi
273 for 72 hours after a synchronized lay. In contrast to the suppression that we observed upon
274 *mes-4* RNAi, *met-1* RNAi had no effect. By 72 hours, none of the *spr-5; met-2* mutant
275 progeny (0/573) from hermaphrodites fed *met-1* RNAi developed to adults, and these

276 animals were indistinguishable from *spr-5; met-2* progeny fed control RNAi (Figure 6G, I).
277 Additionally, *met-1* RNAi itself had no effect on developmental delay, as nearly all of the N2
278 progeny (715/721) from hermaphrodites fed *met-1* RNAi developed to adults (Figure 6C,
279 I).
280
281 **Knocking down SET-2 rescues *spr-5; met-2* developmental delay**
282 If the developmental delay of *spr-5; met-2* mutants is caused by ectopic inheritance
283 of H3K4me2 driving the expression MES-4 germline genes in somatic tissues, we would
284 expect the developmental delay of *spr-5; met-2* progeny to be dependent upon the H3K4
285 methyltransferase, SET-2. To test this, we monitored the development of progeny of *spr-5;*
286 *met-2* hermaphrodites fed *set-2* RNAi for 72 hours after a synchronized lay. Identical to N2
287 progeny from hermaphrodites fed control RNAi, *set-2* RNAi had no effect on the
288 development of wild-type animals, as all of the N2 progeny from hermaphrodites fed *set-2*
289 RNAi developed to adults by 72 hours (1114/1114) (Figure 6D, I). However, in contrast to
290 *spr-5; met-2* progeny fed control RNAi that were developmentally delayed, most of the
291 progeny from *spr-5; met-2* hermaphrodites fed *set-2* RNAi developed to adults (347/384)
292 (Figure 6H, I, unpaired t-test, $p<0.0001$).
293
294 ***spr-5; met-2* progeny acquire transgene silencing in somatic tissues**
295 The somatic expression of MES-4 germline genes involved in germline transgene
296 silencing (Figure S2C-D) raises the possibility that the somatic tissues in *spr-5; met-2*
297 progeny may acquire the ability to silence transgenes, a function normally restricted to
298 germline cells. To test this, we examined the somatic expression of an extrachromosomal

299 multicopy *let-858* transgene that is normally silenced in the germline by both
300 transcriptional and posttranscriptional germline silencing mechanisms (Kelly and Fire,
301 1998). This analysis was performed in *spr-5; met-2* mutant L2 larvae that were undergoing
302 developmental delay. In N2, most of the L2 progeny (117/132) expressed ubiquitous high
303 levels of LET-858::GFP throughout the entire soma (Figure 7A, B, and K), while the
304 remaining progeny (15/132) expressed what we describe as a "faint" level of expression
305 (Figure 7C, D, and K). In contrast, almost none of the *spr-5; met-2* L2 progeny (2/87)
306 displayed high level of transgene expression that is comparable to the high level seen in
307 most N2 progeny (Figure 7E, F, and K). Instead, the majority of *spr-5; met-2* progeny
308 (64/87) had faint LET-858::GFP expression that is comparable to the faint expression
309 observed in N2 progeny (Figure 7G, H, and K). The remaining 21 *spr-5; met-2* progeny had
310 no LET-858::GFP expression. Because less than 50% of progeny inherited the *let-858*
311 transgene, we normalized the percentage of progeny scored as "off" for LET-858::GFP to
312 the presence of the *let-858* transgene based on genotyping for *gfp* (see methods). For N2,
313 all of the 60 L2 progeny that were scored as "off" failed to inherit the *let-858* transgene,
314 indicating that the transgene is never silenced in N2 progeny (data not shown). However,
315 for *spr-5; met-2* L2 progeny, eight out of 50 progeny that were scored as "off" inherited the
316 *let-858* transgene indicating that the *let-858* transgene can be completely silenced in some
317 *spr-5; met-2* progeny. After normalization for the transgene inheritance, we observed that
318 21/87 of *spr-5; met-2* progeny displayed no visible expression of the LET-858::GFP
319 transgene (Figure 7I, J, and K).
320
321 **DISCUSSION**

322 ***spr-5; met-2* maternal reprogramming prevents developmental delay by restricting**
323 **ectopic MES-4 bookmarking**

324 SPR-5 and MET-2 act maternally to reprogram histone methylation and prevent the
325 transcriptional state of the parent from being inappropriately transmitted to the offspring
326 (Kerr et al., 2014). In this study, we find that the loss of SPR-5 and MET-2 maternal
327 reprogramming led to a severe developmental delay that was associated with the ectopic
328 expression of MES-4 germline genes in somatic tissues. This finding raises the possibility
329 that SPR-5 and MET-2 reprogramming blocks the ectopic expression of MES-4 germline
330 genes by preventing the accumulation of MES-4 dependent H3K36me3 at a subset of
331 germline genes in somatic tissues. Consistent with this possibility, most of the MES-4
332 germline genes were increased in *spr-5; met-2* mutants compared to N2 in L1 larvae. Using
333 smFISH, we also confirmed the somatic expression of two ectopically expressed MES-4
334 germline genes, *htp-1* and *cpb-1*. While *htp-1* mRNA was ectopically detected in many
335 somatic tissues, the ectopic expression of *cpb-1* mRNA was more restricted, suggesting that
336 the extent of ectopic expression is dependent upon the locus.

337 In the absence of SPR-5 and MET-2 reprogramming, MES-4 germline genes
338 accumulated ectopic H3K36me3 in the soma. This suggests that without SPR-5 and MET-2
339 reprogramming, MES-4 ectopically maintains H3K36me3 at these genes in somatic tissues.
340 Of note, we observe a low level of H3K36me3 at germline genes in the somatic tissues of N2
341 progeny. It is unclear why there is a low level of H3K36me3 normally in somatic tissues in
342 N2 animals. Nevertheless, the absence of transcription associated with this low level of
343 H3K36me3 indicates that an increased level of H3K36me3 is necessary to cause ectopic
344 transcription.

345 If the ectopic maintenance of H3K36me3 in the soma of *spr-5; met-2* mutant progeny
346 is causing the developmental delay, then removal of MES-4 should rescue the ectopic
347 expression and developmental delay. Indeed, we find that the removal of MES-4 rescued
348 both the ectopic transcription of MES-4 germline genes in the soma of *spr-5; met-2* progeny,
349 and the developmental delay. Importantly, removing the transcriptionally coupled
350 H3K36me3 methyltransferase, MET-1, did not rescue the developmental delay. Thus, the
351 developmental delay that we observe in *spr-5; met-2* progeny is only dependent on
352 transcriptionally independent H3K36me3. Taken together, our data provide
353 comprehensive evidence that the developmental delay of *spr-5; met-2* progeny is caused by
354 the ectopic expression of MES-4 germline genes.
355
356 **How does an ectopic transcriptional program interfere with developmental timing?**
357 How does the ectopic expression of germline genes interfere with somatic tissues to
358 cause developmental delay? One possibility is that the ectopic expression of MES-4
359 germline genes causes the soma to take on germline character. To begin to address this, we
360 asked whether *spr-5; met-2* double mutants can silence an extrachromosomal array in
361 somatic tissues. The silencing of extrachromosomal arrays is normally restricted to the
362 germline (Kelly and Fire, 1998). However, we find that *spr-5; met-2* progeny acquired some
363 ability to silence an extrachromosomal multicopy array in somatic cells. Consistent with
364 this finding, loss of the somatic repressor LIN-35 also results in the somatic silencing of a
365 GFP transgene (Wang et al., 2005). Intriguingly, in the *spr-5; met-2* mutant RNA-seq we
366 detected the ectopic expression of RNA-dependent RNA polymerase genes (e.g. *rrf-1* and
367 *gld-2*) as well as genes involved in the RNAi effector complex (e.g. *hrde-1* and *ppw-1*). These

368 pathways have previously been implicated in gene silencing (Buckley et al., 2012; Sijen et
369 al., 2001; Tijsterman et al., 2002). Thus, similar to what has been found in *lin-35* mutants
370 (Wang et al., 2005), it is possible that the somatic silencing of the transgene in *spr-5; met-2*
371 mutants is due to the induction of the germline small RNA pathway. In a reciprocal fashion,
372 heritable silencing via small RNAs requires MET-2. This provides a further indication that
373 the chromatin and small RNA pathways may be functioning together (Lev et al., 2017).
374 Normally in L1 larvae, the primordial germ cells, Z2 and Z3, are arrested at the
375 G2/M checkpoint (Fukuyama et al., 2006). In the *spr-5; met-2* mutant RNA-seq, we also
376 detected the ectopic expression of genes involved in the negative regulation of proliferation
377 and the cell cycle, as well as G2/M checkpoint genes. Thus, it is also possible that ectopic
378 expression of germline genes normally expressed only in Z2 and Z3 contributes to the
379 developmental delay through the ectopic activation of germline cell cycle control.
380 Regardless, the silencing of the extrachromosomal multicopy array suggests that the
381 somatic tissues in *spr-5; met-2* progeny make functional proteins that can perform some
382 germline functions. We propose that either ectopic germline transcription, or an ectopic
383 germline function resulting from this ectopic transcription, interferes with the ability of
384 somatic cells to properly enact their transcriptional program. This background noise delays
385 the proper adoption of cell fate, leading to an overall delay in the development of the tissue.
386

387 **A model for how the inheritance of histone methylation is balanced to specify**
388 **germline versus soma**

389 By linking maternal *spr-5; met-2* reprogramming to the MES-4 germline inheritance
390 system, our data provide a rationale for the existence of MES-4 bookmarking, through the

391 following model. In the germline, transcriptional elongation is blocked by PIE-1, which
392 segregates to germline blastomeres during embryogenesis (Batchelder et al., 1999; Mello et
393 al., 1992; Seydoux et al., 1996) (Figure 8A, B). In the soma of the early embryo, there is also
394 very little transcription, because the bulk of zygotic transcription does not begin until
395 approximately the 60-cell stage. This stage is just prior to when the primordial germ cells,
396 Z2 and Z3, are specified (Sulston et al., 1983). Thus, in *C. elegans,* germline versus soma is
397 largely specified without transcription.

398 During normal maternal reprogramming, SPR-5 and MET-2 are deposited into the
399 oocyte. At fertilization they facilitate the reprogramming of previously expressed genes
400 from an active chromatin state to a repressed chromatin state by removing H3K4me2 and
401 adding H3K9me2 (Kerr et al., 2014) (Figure 8A). This reprogramming is necessary to
402 prevent the transcriptional memory of the previous generation from being inappropriately
403 propagated to the progeny. Genes epigenetically reprogrammed by SPR-5 and MET-2
404 include ubiquitously expressed genes and germline expressed genes, a subset of which are
405 MES-4 germline genes. The MES-4 germline genes are subsequently targeted by the
406 transcription independent H3K36 methyltransferase, MES-4, to maintain H3K36me3 in the
407 germ lineage during embryogenesis (Figure 8A, B). We propose that H3K36 methylation
408 bookmarking antagonizes the repression caused by the erasure of H3K4me2 and the
409 addition of H3K9me2. Without the transcription independent maintenance of inherited
410 H3K36 methylation from the mother to antagonize this repression, the germline fails to
411 proliferate and animals are sterile (Capowski et al., 1991; Garvin et al., 1998). The failure to
412 proliferate and sterility caused by loss of MES-4 is presumably because germline genes that
413 are targeted by MES-4 fail to reactivate, though it has yet to be demonstrated. Thus, our

414 data suggest that the MES-4 bookmarking system is necessary for critical germline genes to
415 bypass the global epigenetic reprogramming that occurs at fertilization to prevent
416 transgenerational inheritance. We refer to this initial phase of filtering inherited histone
417 methylation at fertilization as the establishment phase.

418 Following this establishment phase, a maintenance phase is required to propagate
419 this initial pattern of histone methylation throughout embryogenesis. The MES-4
420 bookmarking system is localized primarily to the primordial germ cells in later embryonic
421 development (Furuhashi et al., 2010; Rechtsteiner et al., 2010). This concentration of MES-
422 4 to the germline helps to maintain MES-4 bookmarking for germline specification later in
423 embryonic development. However, MES-4 is also present in somatic tissues (Furuhashi et
424 al., 2010; Rechtsteiner et al., 2010). This makes the system vulnerable to the ectopic
425 maintenance of MES-4 bookmarking in the soma. For this reason, multiple systems, such as
426 LIN-15B and LIN-35, as well as MEP-1 and LET-418, function in somatic tissues to restrict
427 H3K36 bookmarking by MES-4 to the germline. Thus, in the maintenance phase, the
428 balance of MES-4 and the systems that somatically antagonize MES-4, maintain the histone
429 methylation pattern that is initiated during the establishment phase. Taken together, we
430 propose that SPR-5, MET-2 and MES-4 carefully balance the inheritance of three different
431 histone modifications, H3K4, H3K9, and H3K36 methylation, to ensure the proper
432 specification of germline versus soma in the absence of transcription.

433 The model that we have proposed makes the following two predictions. First, MES-4
434 germline genes should normally be targeted for continued silencing by H3K9me2 in
435 somatic tissues. It has recently been shown that a subset of germline specific genes contain
436 H3K9me2 at their promoters in somatic tissues (Rechtsteiner et al., 2019). We re-examined

437 the H3K9me2 ChIP-seq dataset from this work and found that the MES-4 germline genes
438 that are ectopically expressed in the somatic tissues of *spr-5; met-2* progeny also displayed
439 unique H3K9me2 promoter peaks. This confirms that MES-4 germline genes are normally
440 repressed by H3K9me2 in somatic tissues.

441 The second prediction from our model is that the ectopic inheritance of H3K4
442 methylation at MES-4 germline genes overwhelms the somatic repression systems. Despite
443 the presence of these transcriptional repressor complexes and chromatin remodelers to
444 antagonize MES-4 bookmarking in the soma, loss of *spr-5; met-2* maternal reprogramming
445 results in the somatic expression of MES-4 germline genes. This suggests that the failure to
446 add H3K9me2, as well as the inappropriate retention of H3K4me2, results in a chromatin
447 environment that is permissive for the ectopic maintenance of H3K36me3 in the soma,
448 even in the presence of the systems that repress MES-4 bookmarking somatically (Figure
449 8B). If this is the case, then the developmental delay in *spr-5; met-2* progeny should also be
450 dependent upon the activity of the H3K4 methyltransferase. We find that knocking down
451 SET-2, the H3K4me1/2 methyltransferase, rescued the developmental delay that we
452 observe in *spr-5; met-2* progeny. These findings suggest that the inheritance of ectopic
453 H3K4 methylation enables the ectopic accumulation of MES-4 dependent H3K36me3, and
454 the subsequent ectopic expression of MES-4 germline genes in somatic tissues of *spr-5;*
455 *met-2* progeny. It is not entirely clear how the subsequent ectopic maintenance of
456 H3K36me3 facilitates ectopic expression. However, it should be noted that there were
457 some differences in which MES-4 germline genes were ectopically expressed between our
458 two *spr-5; met-2* RNA-seq experiments. This stochasticity is consistent with H3K36me3
459 being permissive, rather than instructive, for transcription. If this is the case, it is doubtful

460 that the *spr-5; met-2* developmental delay is caused by the inappropriate expression of any
461 single MES-4 germline gene. Rather, it is likely that the developmental delay is caused by
462 either the inappropriate expression of multiple MES-4 germline genes, or the ectopic
463 activation of the MES-4 germline program.
464

465 **Conservation of maternal epigenetic reprogramming between invertebrates and**
466 **vertebrates**

467 Epigenetic reprogramming at fertilization is a problem that all sexually reproducing
468 organisms must solve (Lee and Katz, 2020). Thus, it is possible that the mechanisms of
469 epigenetic reprogramming may be conserved. Along with the Heard lab, we previously
470 demonstrated that progeny from mice that maternally lack the vertebrate SPR-5 homolog,
471 KDM1A/LSD1, ectopically maintain the expression of germline genes in the embryo. This
472 causes embryonic lethality at the two-cell stage (Ancelin et al., 2016; Wasson et al., 2016).
473 Similarly, maternal loss of the MET-2 ortholog SETDB1 or the MES-4 ortholog NSD1 in mice
474 results in early embryonic lethality (J. Kim et al., 2016; Rayasam et al., 2003). Together
475 these results underscore the developmental importance of properly regulating histone
476 methylation between generations and raise the possibility that the mechanism we have
477 uncovered is conserved in mammals.

478 The model that we have proposed may also help explain the mechanism underlying
479 patients harboring mutations in various histone-modifying enzymes. Recent genome
480 sequencing has revealed that several neurodevelopmental disorders are caused by
481 mutations in histone modifying enzymes (extensively reviewed by (J.-H. Kim et al., 2017).
482 These include mutations in: 1) the H3K36 methyltransferase *Setd2* and the H3K27

483 demethylase *Kdm6a,* which cause Kabuki Syndrome (Lederer et al., 2012), 2) the human
484 ortholog of *spr-5, Lsd1,* which causes a Kabuki-like Syndrome (Chong et al., 2016; Tunovic
485 et al., 2014), and 3) the H3K36 methyltransferase *Nsd1* which causes Sotos Syndrome
486 (Kurotaki et al., 2002). Similar to what we observed in *spr-5; met-2* mutant progeny, many
487 of the human patients with mutations in these histone modifying enzymes suffer from
488 global developmental delay. Based on our model, it is possible that the developmental
489 delay in these patients may be caused by the failure to properly regulate histone
490 methylation during critical developmental transitions. The resulting inappropriate
491 inheritance of histone methylation could result in the ectopic expression of a
492 developmental program in an inappropriate tissue, leading to background noise and
493 developmental delay.
494

495 **MATERIALS AND METHODS**

496 **Strains.** All *Caenorhabditis elegans strains* were grown and maintained at 20° C under
497 standard conditions, as previously described (Brenner, 1974). The *C. elegans spr-5*
498 *(by101)(I)* strain was provided by R. Baumeister. The N2 Bristol wild-type (WT) strain was
499 provided by the *Caenorhabditis* Genetics Center. The *met-2 (n4256)(III) strain* was provided
500 by R. Horvitz. The *hT2 [bli-4(e937)let-?(q782)qls48] (I;III)* balancer strain was used to
501 maintain *spr-5 (by101)(I); met-2 (n4256)(III)* double-mutant animals as heterozygotes.
502 Because the *hT2 [bli-4(e937)let-?(q782)qls48](I;III)* balancer allele does not extend
503 completely to the *spr-5* locus on chromosome I, the F0 animals used to generate F1 *spr-5;*
504 *met-2* progeny were cloned out and genotyped to confirm the presence of the *spr-5*
505 *(by101)(I)* allele. For genotyping, single animals were picked into 5-10ul of lysis buffer

506 (50mM KCl, 10mM Tris-HCl (pH 8.3), 2.5mM $MgCl_2$, 0.45% NP-40, 0.45% Tween-20, 0.01%
507 gelatin) and incubated at 65°C for 1 hour followed by 95°C for 30 minutes. PCR reactions
508 were performed with AmpliTaq Gold (Invitrogen) according to the manufacturer's protocol
509 and reactions were resolved on agarose gels (see supplementary file 5 for primer
510 sequences). Before completing this study we acquired the FX30208 *tmC27 [unc-*
511 *75(tmls1239*)](I) from the *Caenorhabditis* Genetics Center that completely covers the *spr-5*
512 locus on chromosome I. The *qC1 [qls26 (lag2::GFP + rol-6(su1006)](III)* strain was obtained
513 from W. Kelly and crossed to *met-2 (n4256)(III)* to maintain *met-2(n4256)(III)* as
514 heterozygotes. The *spr-5 (by101)(I)/tmC27[unc-75(tmls1239)](I); met-2 (n4256) (III*)/qC1
515 [qls26 (lag2::gfp+ rol-6(su1006))](III) strain was then re-created for this study to maintain
516 *spr-5 (by101)(I); met-2 (n4256)(III)* double-mutant animals as balanced heterozygotes. The
517 LET-858::GFP (*pha-1*(e2123ts)(III); *let-858::gfp* (ccEx7271)) (Kelly and Fire, 1998)
518 transgenic strain used in somatic transgene silencing assays was acquired from W. Kelly.
519 **Scoring developmental delay.** *C. elegans* adult hermaphrodites were allowed to lay
520 embryos for 2-4 hours and then removed in order to synchronize the development of
521 progeny. Progeny were then imaged and scored for development to the adult stage at
522 either 72 hours or seven days after synchronized lay, depending on the experiment.
523 **RNA sequencing and analysis.** Total RNA was isolated using TRIzol reagent (Invitrogen)
524 from 200-250 starved L1 larvae born at room temperature (21°C - 22°C) overnight in M9
525 Buffer. Due to difficulty in isolating large numbers of *spr-5; met-2* double-mutant progeny
526 from the *hT2 [bli-4(e937)let-?(q782)qls48](I;III)* balancer strain, we submitted total RNA to
527 the Genomic Services Laboratory (GSL) (HudsonAlpha, Huntsville, Alabama) for low input
528 RNA-seq services. This service utilizes the Ovation RNA-Seq System V2 kit (Nugen) for

529 initial RNA amplification prior to library preparation and sequencing (Illumina HiSeq v4,
530 50bp paired-end reads). For each genotype, 2 biological replicates were obtained. During
531 the course of these experiments, the FX30208 *tmC27 [unc-75(tmls1239)]*(I) balancer
532 became available from the *Caenorhabditis* Genetics Center. This balancer completely covers
533 the *spr-5* locus on chromosome I. Using this balanced strain, we performed a repeat *spr-5;*
534 *met-2* RNA-seq experiment with three additional biological replicates of *spr-5; met-2* versus
535 N2 L1 progeny. We submitted the total RNA from new replicates of the repeat RNA-seq to
536 Georgia Genomics and Bioinformatics Core (University of Georgia, Athens, Georgia) for
537 standard Poly-A RNA-seq services (Illumina Nextseq, 50bp paired-end reads). Downstream
538 quality control and analysis were performed identically for both RNA-seq experiments. For
539 both the low-input and repeat standard RNA-seq, sequencing reads were checked for
540 quality using FastQC (Wingett and Andrews, 2018), filtered using Trimmomatic (Bolger et
541 al., 2014), and remapped to the *C. elegans* transcriptome (ce10, WS220) using HISAT2 (D.
542 Kim et al., 2015). Read count by gene was obtained by FeatureCounts (Liao et al., 2014).
543 Differentially expressed transcripts for the low-input RNA-seq experiment (significance
544 threshold, Wald test, p-value < 0.05) and the repeat RNA-seq experiment (significance
545 threshold, Wald test, p-adj < 0.05) were determined using DESEQ2 (v.2.11.40.2) (Love et
546 al., 2014). Transcripts per million (TPM) values were calculated from raw data obtained
547 from FeatureCounts output. Subsequent downstream analysis was performed using R with
548 normalized counts and p-values from DESEQ2 (v.2.11.40.2). Heatmaps were produced
549 using the ComplexHeatmap R Package (Gu et al., 2016). Data was scaled and hierarchical
550 clustering was performed using the complete linkage algorithm. In the linkage algorithm,
551 distance was measured by calculating pairwise distance. Volcano plots were produced

552 using the EnhancedVolcano package (v.0.99.16). Additionally, Gene Ontology (GO) Pathway
553 analysis was performed using the online platform WormEnrichr (Chen et al., 2013;
554 Kuleshov et al., 2016). Rechtsteiner and colleagues identified 214 MES-4 germline genes
555 (Rechtsteiner et al., 2010). 17 of these genes are pseudogenes that we were unable to
556 convert from Ensembl transcript IDs to RefSeq mRNA accession, and another gene was
557 duplicated, so we removed those genes. This leaves 196 MES-4 germline genes that we
558 used for our analysis. An additional heatmap comparison of differentially expressed genes
559 between *spr-5*, *met-2*, and *spr-5; met-2* progeny compared to N2 progeny was generated in
560 Microsoft Excel using log2 fold change values from the DESEQ2 analysis. Because transcript
561 isoforms were ignored, we discuss the data in terms of "genes expressed" rather than
562 "transcripts expressed".
563 **Chromatin immunoprecipitation sequencing and analysis.** Chromatin
564 immunoprecipitation (ChIP) experiments were performed as described by Katz and
565 colleagues (Katz et al., 2009). Briefly, 600 starved L1 larvae born at room temperature
566 (21°C - 22°C) overnight in M9 Buffer were collected, frozen in liquid nitrogen, and stored at
567 -80°C prior to homogenization. Frozen pellets were disrupted by a glass Dounce
568 homogenizer, fixed with formaldehyde (1% final concentration), and quenched with
569 glycine. ChIP samples were processed with a Chromatin Immunoprecipitation Assay Kit
570 (Millipore), according to manufacturer's instructions. Samples were sonicated using a
571 Diagenode Bioruptor UCD-200 at 4°C on the "high" setting for a total of 30min with a cycle
572 of 45sec on and 15sec off. A total of 12.5µL (5ug) H3K36me3 antibody (cat. 61021; Active
573 motif) was used for immunoprecipitation. The Genomic Services Laboratory (GSL)
574 (HudsonAlpha, Huntsville, Alabama) performed library preparation and sequencing

575 (Illumina HiSeq v4, 50bp single-end reads). Reads were checked for quality using FastQC
576 (Wingett and Andrews, 2018) and remapped to the *C. elegans* transcriptome (ce10, WS220)
577 using Bowtie2 (Langmead and Salzberg, 2012; Langmead et al., 2009) under default
578 parameters. bamCoverage in deepTools2 (Ramírez et al., 2016) was used to generate
579 bigwig coverage tracks in 50bp bins, with blacklisted regions from McMurchy et al. 2017
580 excluded, using the following parameters: -bs 50, --normalizeUsing RPKM (McMurchy et al.,
581 2017). MACS2 (Feng et al., 2012; Zhang et al., 2008) default parameters were used to call
582 peaks and create bedgraph files for sequenced and mapped H3K36me3 ChIP samples and
583 input DNA samples with the following adjustments to account for H3K36me3 broader
584 domains: Broad-cutoff =0.001. Blacklisted regions from McMurchy et al. 2017 were
585 excluded for this analysis (McMurchy et al., 2017). Using published H3K36me3 modMine
586 Chip-chip called broad peaks (modENCODE_3555) from N2 L1 larvae as a guide, we then
587 merged called broad peaks within 1200bp using Bedtools: MergeBED (Quinlan and Hall,
588 2010). H3K9me2 bedgraph files used in our analysis were from a published dataset
589 (Rechtsteiner et al., 2019). Integrative Genome Viewer (IGV) was used to visualize
590 H3K36me3 reads normalized to reads per kilobase millions (RPKM) and H3K9me2 reads
591 normalized to 15 million reads (genome wide coverage of H3K9me2; (Rechtsteiner et al.,
592 2019).
593 **RNAi methods.** RNAi by feeding was carried out using clones from the Ahringer library
594 (Kamath and Ahringer, 2003). Feeding experiments were performed on RNAi plates (NGM
595 plates containing 100 ug/ml ampicillin, 0.4mM IPTG, and 12.5ug/ml tetracycline). F0
596 worms were placed on RNAi plates as L2 larvae and then moved to fresh RNAi plates 48hrs
597 later where they were allowed to lay embryos for 2-4 hrs. F0 worms were then removed

598 from plates and sacrificed or placed in M9 buffer overnight so that starved L1 progeny
599 could be isolated for quantitative PCR (qPCR). F1 progeny were scored 72hrs after the
600 synchronized lay for developmental progression. For each RNAi experiment, *pos-1* RNAi
601 was used as a positive control. Each RNAi experiment reported here *pos-1* RNAi resulted in
602 >95% embryonic lethality, indicating that RNAi plates were optimal.
603 **Real-time expression analysis.** Total RNA was isolated using TRIzol reagent (Invitrogen)
604 from synchronized L1s born at room temperature (21°C – 22°C). cDNA synthesis and qPCR
605 were carried out as described (Kerr et al. 2014). A total of two biological replicates were
606 performed and for both biological replicates experiments were performed in triplicate and
607 normalized to *ama-1* mRNA expression (see supplementary file 5 for primer sequences).
608 **Differential interference contrast microscopy.** Worms were immobilized in 0.1%
609 levamisole and placed on a 2% agarose pad for imaging at either 10x or 40x magnification.
610 40x DIC images were overlaid together using Adobe photoshop to generate high resolution
611 images of whole worms.
612 **Single Molecule Fluorescent *in situ* Hybridization (smFISH).** Quasar 570 labeled
613 smFISH probe sets for *htp-1* and *cpb-1* were designed using Stellaris Probe Designer
614 (Biosearch) (see supplementary file 4 for probe sequences). The *htp-1* smFISH probes were
615 designed using the complete 1,059nt *htp-1* protein-coding sequence. Likewise, The *cpb-1*
616 smFISH probes were designed using the complete 1,683nt *cpb-1* protein-coding sequence.
617 In addition, an smFISH fluorescent probe set for *ama-1* was purchased from the
618 DesignReady catalog (cat#: VSMF-6002-5, Biosearch). Synchronized L1 larvae for smFISH
619 were obtained by bleaching 300-500 gravid hermaphrodites and allowing embryos to
620 hatch overnight on 6cm NGM plates lightly seeded OP50 bacteria. L1 larvae were then

621 washed into 1.5ul Eppendorf tubes using nuclease-free M9 buffer. Fixation and
622 hybridization steps followed the Stellaris RNA FISH protocol for *C. elegans* adapted from
623 RAJ lab protocol (Raj and Tyagi, 2010). In brief, we resuspended L1 larvae in fixation buffer
624 (3.7% formaldehyde in 1 x PBS) for 15 minutes at room temperature then transferred
625 tubes to liquid nitrogen. Samples were thawed in water and placed on ice for 20 minutes. In
626 our hands, we obtain better fluorescent signal by freeze cracking L1 larvae. Following
627 fixation, L1 Larvae were resuspended in 70% EtOH and stored at 4°C for 24-48 hours. For
628 all probe sets, we incubated L1 larvae in 100ul hybridization buffer (containing 10%
629 formamide and 125nm probe) for 4 hours at 37°C. After hybridization, samples were
630 washed in wash buffer at 37°C for 30 minutes, incubated in 50ng/mL DAPI in wash buffer
631 at 30°C for 30 minutes, washed once in 2x SSC for 2 minutes at room temperature, and
632 mounted in Vectashield mounting medium. Mounted slides were imaged immediately using
633 a 100x objective on a spinning-disk confocal Nikon-TiE imaging system. Images were
634 captured using NIS-Elements software (Nikon) and ImageJ (NIH, http://imagej.nih.gov/ij/)
635 was used for viewing. ImageJ maximum projection was used to project z-stack images to a
636 single plane. The fluorescent intensity of smFISH dots were > 2-fold above background as
637 expected (Ji and van Oudenaarden, 2012).
638 **LET-858::GFP transgene silencing assay.** First generation *spr-5; met-2* hermaphrodites
639 were crossed to *let-858* transgenic males to generate *spr-5/+*; *met-2/+*; *let-858::gfp* animals.
640 The let-858 transgene is an extrachromosomal multicopy *let-858* array (Kelly and Fire,
641 1998). From these animals we generated *spr-5; met-2; let-858::gfp* animals and scored them
642 for somatic expression of LET-858::GFP using a standard stereoscope. L2 progeny from N2
643 and *spr-5; met-2* progeny expressing the LET-858::GFP transgene were scored as "bright"

644 (High level ubiquitous expression) , faint (barely visible and ubiquitous expression), or off
645 (no expression). Because less than 50% of progeny inherit the *let-858* transgene, we
646 normalized the percentage of progeny scored as "off" for LET-858::GFP to presence of the
647 *let-858* transgene based on genotyping for *gfp.* For N2, 0 out of 60 progeny that were
648 scored as "off" failed to inherit the *let-858* transgene indicating that the transgene is never
649 silenced in N2 progeny (data not shown, see supplementary file 5 for primer sequences).
650 For *spr-5; met-2* progeny, 8 out of 50 progeny that were scored as "off" inherited the *let-858*
651 transgene indicating that the *let-858* transgene is completely silenced in some *spr-5; met-2*
652 progeny (data not shown).
653

654 **ACKNOWLEDGEMENTS**

655 We are grateful to members of the Katz lab, as well as T. Caspary and C. Bean, for their
656 helpful discussion and critical reading of the manuscript; M. J. Rowley for advice on
657 bioinformatics; S. Strome and L. Petrella for helpful discussion and experimental advice; D.
658 Lerit, R. Deal, V. Corces, and W. Kelly for the generous sharing of reagents and equipment.
659 We thank R. Horvitz, W. Kelly, and the *Caenorhabditis* Genetics Center (funded by NIH P40
660 OD010440) for strains. **Funding:** This work was funded by a grant to D.J.K. (NSF
661 IOS1931697); T.W.L. and B.S.C. were supported by the Fellowships in Research and Science
662 Teaching IRACDA postdoctoral program (NIH K12GM00680-15); and B.S.C. was also
663 supported by NIH F32 GM126734-01. **Author Contributions:** B.S.C. and D.J.K. conceived
664 and designed the study and wrote the manuscript. B.S.C. performed experiments under the
665 direction of D.J.K. B.S.C and D.J.K. analyzed data and interpreted results, with help from
666 T.W.L. J.S.B. initially performed *set-2* RNAi rescue experiment and C.F.P. initially performed

667 the *let-858* transgene silencing experiment. D.A.M. helped with RNA-seq analysis. All
668 authors discussed the results. **Data availability**: Raw and processed genomic data has
669 been deposited with the Gene Expression Omnibus (www.ncbi.nlm.nih.gov/geo) under
670 accession code GSE143839.
671

672 **Supplementary Material**

673 Figure Supplements:

674 Figure 1-figure supplement 1

675 Figure 2-figure supplements 1, 2, and 3

676 Figure 3-figure supplement 1

677 Figure 4-figure supplements 1 and 2

678 Supplementary files 1-6

679 Source Data files 1-3

680

681 **REFERENCES**

682 Ancelin, K., Syx, L., Borensztein, M., Ranisavljevic, N., Vassilev, I., Briseño-Roa, L., Liu, T.,
683 Metzger, E., Servant, N., Barillot, E., Chen, C.-J., Schüle, R., Heard, E., 2016. Maternal
684 LSD1/KDM1A is an essential regulator of chromatin and transcription landscapes
685 during zygotic genome activation. Elife 5, 4615. doi:10.7554/eLife.08851
686 Batchelder, C., Dunn, M.A., Choy, B., Suh, Y., Cassie, C., Shim, E.Y., Shin, T.H., Mello, C.,
687 Seydoux, G., Blackwell, T.K., 1999. Transcriptional repression by the Caenorhabditis
688 elegans germ-line protein PIE-1. Genes Dev. 13, 202–212. doi:10.1101/gad.13.2.202
689 Bolger, A.M., Lohse, M., Usadel, B., 2014. Trimmomatic: a flexible trimmer for Illumina
690 sequence data. Bioinformatics 30, 2114–2120. doi:10.1093/bioinformatics/btu170
691 Brenner, S., 1974. The genetics of Caenorhabditis elegans. Genetics 77, 71–94.
692 Buckley, B.A., Burkhart, K.B., Gu, S.G., Spracklin, G., Kershner, A., Fritz, H., Kimble, J., Fire, A.,
693 Kennedy, S., 2012. A nuclear Argonaute promotes multigenerational epigenetic
694 inheritance and germline immortality. Nature 489, 447–451. doi:10.1038/nature11352
695 Capowski, E.E., Martin, P., Garvin, C., Strome, S., 1991. Identification of grandchildless loci
696 whose products are required for normal germ-line development in the nematode
697 Caenorhabditis elegans. Genetics 129, 1061–1072.

698 Chen, E.Y., Tan, C.M., Kou, Y., Duan, Q., Wang, Z., Meirelles, G.V., Clark, N.R., Ma'ayan, A.,
699 2013. Enrichr: interactive and collaborative HTML5 gene list enrichment analysis tool.
700 BMC Bioinformatics 14, 128. doi:10.1186/1471-2105-14-128
701 Chong, J.X., Yu, J.-H., Lorentzen, P., Park, K.M., Jamal, S.M., Tabor, H.K., Rauch, A., Saenz, M.S.,
702 Boltshauser, E., Patterson, K.E., Nickerson, D.A., Bamshad, M.J., 2016. Gene discovery for
703 Mendelian conditions via social networking: de novo variants in KDM1A cause
704 developmental delay and distinctive facial features. Genet. Med. 18, 788–795.
705 doi:10.1038/gim.2015.161
706 Feng, J., Liu, T., Qin, B., Zhang, Y., Liu, X.S., 2012. Identifying ChIP-seq enrichment using
707 MACS. Nat Protoc 7, 1728–1740. doi:10.1038/nprot.2012.101
708 Fukuyama, M., Rougvie, A.E., Rothman, J.H., 2006. C. elegans DAF-18/PTEN mediates
709 nutrient-dependent arrest of cell cycle and growth in the germline. Curr. Biol. 16, 773–
710 779. doi:10.1016/j.cub.2006.02.073
711 Furuhashi, H., Takasaki, T., Rechtsteiner, A., Li, T., Kimura, H., Checchi, P.M., Strome, S.,
712 Kelly, W.G., 2010. Trans-generational epigenetic regulation of C. elegans primordial
713 germ cells. Epigenetics Chromatin 3, 15. doi:10.1186/1756-8935-3-15
714 Garvin, C., Holdeman, R., Strome, S., 1998. The phenotype of mes-2, mes-3, mes-4 and mes-
715 6, maternal-effect genes required for survival of the germline in Caenorhabditis
716 elegans, is sensitive to chromosome dosage. Genetics 148, 167–185.
717 Gu, Z., Eils, R., Schlesner, M., 2016. Complex heatmaps reveal patterns and correlations in
718 multidimensional genomic data. Bioinformatics 32, 2847–2849.
719 doi:10.1093/bioinformatics/btw313
720 Jambhekar, A., Dhall, A., Shi, Y., 2019. Roles and regulation of histone methylation in animal
721 development. Nat. Rev. Mol. Cell Biol. 20, 625–641. doi:10.1038/s41580-019-0151-1
722 Ji, N., van Oudenaarden, A., 2012. Single molecule fluorescent in situ hybridization
723 (smFISH) of C. elegans worms and embryos. WormBook 1–16.
724 doi:10.1895/wormbook.1.153.1
725 Kamath, R.S., Ahringer, J., 2003. Genome-wide RNAi screening in Caenorhabditis elegans.
726 Methods 30, 313–321. doi:10.1016/s1046-2023(03)00050-1
727 Katz, D.J., Edwards, T.M., Reinke, V., Kelly, W.G., 2009. A C. elegans LSD1 demethylase
728 contributes to germline immortality by reprogramming epigenetic memory. Cell 137,
729 308–320. doi:10.1016/j.cell.2009.02.015
730 Kelly, W.G., Fire, A., 1998. Chromatin silencing and the maintenance of a functional
731 germline in Caenorhabditis elegans. Development 125, 2451–2456.
732 Kerr, S.C., Ruppersburg, C.C., Francis, J.W., Katz, D.J., 2014. SPR-5 and MET-2 function
733 cooperatively to reestablish an epigenetic ground state during passage through the
734 germ line. Proc. Natl. Acad. Sci. U.S.A. 111, 9509–9514. doi:10.1073/pnas.1321843111
735 Kim, D., Langmead, B., Salzberg, S.L., 2015. HISAT: a fast spliced aligner with low memory
736 requirements. Nat. Methods 12, 357–360. doi:10.1038/nmeth.3317
737 Kim, J., Zhao, H., Dan, J., Kim, S., Hardikar, S., Hollowell, D., Lin, K., Lu, Y., Takata, Y., Shen, J.,
738 Chen, T., 2016. Maternal Setdb1 Is Required for Meiotic Progression and
739 Preimplantation Development in Mouse. PLoS Genet. 12, e1005970.
740 doi:10.1371/journal.pgen.1005970
741 Kim, J.-H., Lee, J.H., Lee, I.-S., Lee, S.B., Cho, K.S., 2017. Histone Lysine Methylation and
742 Neurodevelopmental Disorders. Int J Mol Sci 18, 1404. doi:10.3390/ijms18071404

743 Kreher, J., Takasaki, T., Cockrum, C., Sidoli, S., Garcia, B.A., Jensen, O.N., Strome, S., 2018.
744 Distinct Roles of Two Histone Methyltransferases in Transmitting H3K36me3-Based
745 Epigenetic Memory Across Generations in Caenorhabditis elegans. Genetics 210, 969–
746 982. doi:10.1534/genetics.118.301353
747 Kuleshov, M.V., Jones, M.R., Rouillard, A.D., Fernandez, N.F., Duan, Q., Wang, Z., Koplev, S.,
748 Jenkins, S.L., Jagodnik, K.M., Lachmann, A., McDermott, M.G., Monteiro, C.D., Gundersen,
749 G.W., Ma'ayan, A., 2016. Enrichr: a comprehensive gene set enrichment analysis web
750 server 2016 update. Nucleic Acids Res. 44, W90–7. doi:10.1093/nar/gkw377
751 Kurotaki, N., Imaizumi, K., Harada, N., Masuno, M., Kondoh, T., Nagai, T., Ohashi, H.,
752 Naritomi, K., Tsukahara, M., Makita, Y., Sugimoto, T., Sonoda, T., Hasegawa, T., Chinen,
753 Y., Tomita Ha, H.-A., Kinoshita, A., Mizuguchi, T., Yoshiura Ki, K.-I., Ohta, T., Kishino, T.,
754 Fukushima, Y., Niikawa, N., Matsumoto, N., 2002. Haploinsufficiency of NSD1 causes
755 Sotos syndrome. Nat. Genet. 30, 365–366. doi:10.1038/ng863
756 Langmead, B., Salzberg, S.L., 2012. Fast gapped-read alignment with Bowtie 2. Nat. Methods
757 9, 357–359. doi:10.1038/nmeth.1923
758 Langmead, B., Trapnell, C., Pop, M., Salzberg, S.L., 2009. Ultrafast and memory-efficient
759 alignment of short DNA sequences to the human genome. Genome Biol. 10, R25.
760 doi:10.1186/gb-2009-10-3-r25
761 Lederer, D., Grisart, B., Digilio, M.C., Benoit, V., Crespin, M., Ghariani, S.C., Maystadt, I.,
762 Dallapiccola, B., Verellen-Dumoulin, C., 2012. Deletion of KDM6A, a histone
763 demethylase interacting with MLL2, in three patients with Kabuki syndrome. Am. J.
764 Hum. Genet. 90, 119–124. doi:10.1016/j.ajhg.2011.11.021
765 Lee, T.W., Katz, D.J., 2020. Hansel, Gretel, and the Consequences of Failing to Remove
766 Histone Methylation Breadcrumbs. Trends Genet. 36, 160–176.
767 doi:10.1016/j.tig.2019.12.004
768 Lev, I., Seroussi, U., Gingold, H., Bril, R., Anava, S., Rechavi, O., 2017. MET-2-Dependent H3K9
769 Methylation Suppresses Transgenerational Small RNA Inheritance. Curr. Biol. 27,
770 1138–1147. doi:10.1016/j.cub.2017.03.008
771 Liao, Y., Smyth, G.K., Shi, W., 2014. featureCounts: an efficient general purpose program for
772 assigning sequence reads to genomic features. Bioinformatics 30, 923–930.
773 doi:10.1093/bioinformatics/btt656
774 Love, M.I., Huber, W., Anders, S., 2014. Moderated estimation of fold change and dispersion
775 for RNA-seq data with DESeq2. Genome Biol. 15, 550. doi:10.1186/s13059-014-0550-8
776 McMurchy, A.N., Stempor, P., Gaarenstroom, T., Wysolmerski, B., Dong, Y., Aussianikava, D.,
777 Appert, A., Huang, N., Kolasinska-Zwierz, P., Sapetschnig, A., Miska, E.A., Ahringer, J.,
778 2017. A team of heterochromatin factors collaborates with small RNA pathways to
779 combat repetitive elements and germline stress. Elife 6, 7931. doi:10.7554/eLife.21666
780 Mello, C.C., Draper, B.W., Krause, M., Weintraub, H., Priess, J.R., 1992. The pie-1 and mex-1
781 genes and maternal control of blastomere identity in early C. elegans embryos. Cell 70,
782 163–176. doi:10.1016/0092-8674(92)90542-k
783 Petrella, L.N., Wang, W., Spike, C.A., Rechtsteiner, A., Reinke, V., Strome, S., 2011. synMuv B
784 proteins antagonize germline fate in the intestine and ensure C. elegans survival.
785 Development 138, 1069–1079. doi:10.1242/dev.059501
786 Quinlan, A.R., Hall, I.M., 2010. BEDTools: a flexible suite of utilities for comparing genomic
787 features. Bioinformatics 26, 841–842. doi:10.1093/bioinformatics/btq033

788 Raj, A., Tyagi, S., 2010. Detection of individual endogenous RNA transcripts in situ using
789 multiple singly labeled probes. Meth. Enzymol. 472, 365–386. doi:10.1016/S0076-
790 6879(10)72004-8
791 Ramírez, F., Ryan, D.P., Grüning, B., Bhardwaj, V., Kilpert, F., Richter, A.S., Heyne, S., Dündar,
792 F., Manke, T., 2016. deepTools2: a next generation web server for deep-sequencing data
793 analysis. Nucleic Acids Res. 44, W160–5. doi:10.1093/nar/gkw257
794 Rayasam, G.V., Wendling, O., Angrand, P.-O., Mark, M., Niederreither, K., Song, L., Lerouge, T.,
795 Hager, G.L., Chambon, P., Losson, R., 2003. NSD1 is essential for early post-implantation
796 development and has a catalytically active SET domain. EMBO J. 22, 3153–3163.
797 doi:10.1093/emboj/cdg288
798 Rechtsteiner, A., Costello, M.E., Egelhofer, T.A., Garrigues, J.M., Strome, S., Petrella, L.N.,
799 2019. Repression of Germline Genes in Caenorhabditis elegans Somatic Tissues by
800 H3K9 Dimethylation of Their Promoters. Genetics 212, 125–140.
801 doi:10.1534/genetics.118.301878
802 Rechtsteiner, A., Ercan, S., Takasaki, T., Phippen, T.M., Egelhofer, T.A., Wang, W., Kimura, H.,
803 Lieb, J.D., Strome, S., 2010. The histone H3K36 methyltransferase MES-4 acts
804 epigenetically to transmit the memory of germline gene expression to progeny. PLoS
805 Genet. 6, e1001091. doi:10.1371/journal.pgen.1001091
806 Seydoux, G., Mello, C.C., Pettitt, J., Wood, W.B., Priess, J.R., Fire, A., 1996. Repression of gene
807 expression in the embryonic germ lineage of C. elegans. Nature 382, 713–716.
808 doi:10.1038/382713a0
809 Shi, Y., Lan, F., Matson, C., Mulligan, P., Whetstine, J.R., Cole, P.A., Casero, R.A., Shi, Y., 2004.
810 Histone demethylation mediated by the nuclear amine oxidase homolog LSD1. Cell 119,
811 941–953. doi:10.1016/j.cell.2004.12.012
812 Shi, Y.-J., Matson, C., Lan, F., Iwase, S., Baba, T., Shi, Y., 2005. Regulation of LSD1 histone
813 demethylase activity by its associated factors. Mol. Cell 19, 857–864.
814 doi:10.1016/j.molcel.2005.08.027
815 Sijen, T., Fleenor, J., Simmer, F., Thijssen, K.L., Parrish, S., Timmons, L., Plasterk, R.H., Fire, A.,
816 2001. On the role of RNA amplification in dsRNA-triggered gene silencing. Cell 107,
817 465–476. doi:10.1016/s0092-8674(01)00576-1
818 Strome, S., 2005. Specification of the germ line. WormBook 1–10.
819 doi:10.1895/wormbook.1.9.1
820 Sulston, J.E., Schierenberg, E., White, J.G., Thomson, J.N., 1983. The embryonic cell lineage of
821 the nematode Caenorhabditis elegans. Dev. Biol. 100, 64–119. doi:10.1016/0012-
822 1606(83)90201-4
823 Tijsterman, M., Okihara, K.L., Thijssen, K., Plasterk, R.H.A., 2002. PPW-1, a PAZ/PIWI
824 protein required for efficient germline RNAi, is defective in a natural isolate of C.
825 elegans. Curr. Biol. 12, 1535–1540. doi:10.1016/s0960-9822(02)01110-7
826 Tunovic, S., Barkovich, J., Sherr, E.H., Slavotinek, A.M., 2014. De novo ANKRD11 and KDM1A
827 gene mutations in a male with features of KBG syndrome and Kabuki syndrome. Am. J.
828 Med. Genet. A 164A, 1744–1749. doi:10.1002/ajmg.a.36450
829 Unhavaithaya, Y., Shin, T.H., Miliaras, N., Lee, J., Oyama, T., Mello, C.C., 2002. MEP-1 and a
830 homolog of the NURD complex component Mi-2 act together to maintain germline-
831 soma distinctions in C. elegans. Cell 111, 991–1002.

832 Wang, D., Kennedy, S., Conte, D., Kim, J.K., Gabel, H.W., Kamath, R.S., Mello, C.C., Ruvkun, G.,
833 2005. Somatic misexpression of germline P granules and enhanced RNA interference in
834 retinoblastoma pathway mutants. Nature 436, 593–597. doi:10.1038/nature04010
835 Wasson, J.A., Simon, A.K., Myrick, D.A., Wolf, G., Driscoll, S., Pfaff, S.L., Macfarlan, T.S., Katz,
836 D.J., 2016. Maternally provided LSD1/KDM1A enables the maternal-to-zygotic
837 transition and prevents defects that manifest postnatally. Elife 5, 296.
838 doi:10.7554/eLife.08848
839 Wingett, S.W., Andrews, S., 2018. FastQ Screen: A tool for multi-genome mapping and
840 quality control. F1000Res 7, 1338. doi:10.12688/f1000research.15931.2
841 Zhang, Y., Liu, T., Meyer, C.A., Eeckhoute, J., Johnson, D.S., Bernstein, B.E., Nusbaum, C.,
842 Myers, R.M., Brown, M., Li, W., Liu, X.S., 2008. Model-based analysis of ChIP-Seq (MACS).
843 Genome Biol. 9, R137. doi:10.1186/gb-2008-9-9-r137

Figure 1. *spr-5; met-2* mutants display severe developmental delay. 10x Differential Interference Contrast (DIC) images of N2 (A), *spr-5* (B), *met-2* (C), and *spr-5; met-2* progeny (D) 72 hours post synchronized lay. Scale bar: 100µm. (E) Percentage of N2, *spr-5*, *met-2*, and *spr-5; met-2* progeny that reached the adult stage (% Adult Progeny) by 72 hours post synchronized lay. Error bars represent the standard deviation of the mean from three experiments. N= the total number of progeny 20-25 hermaphrodites scored over three experiments.

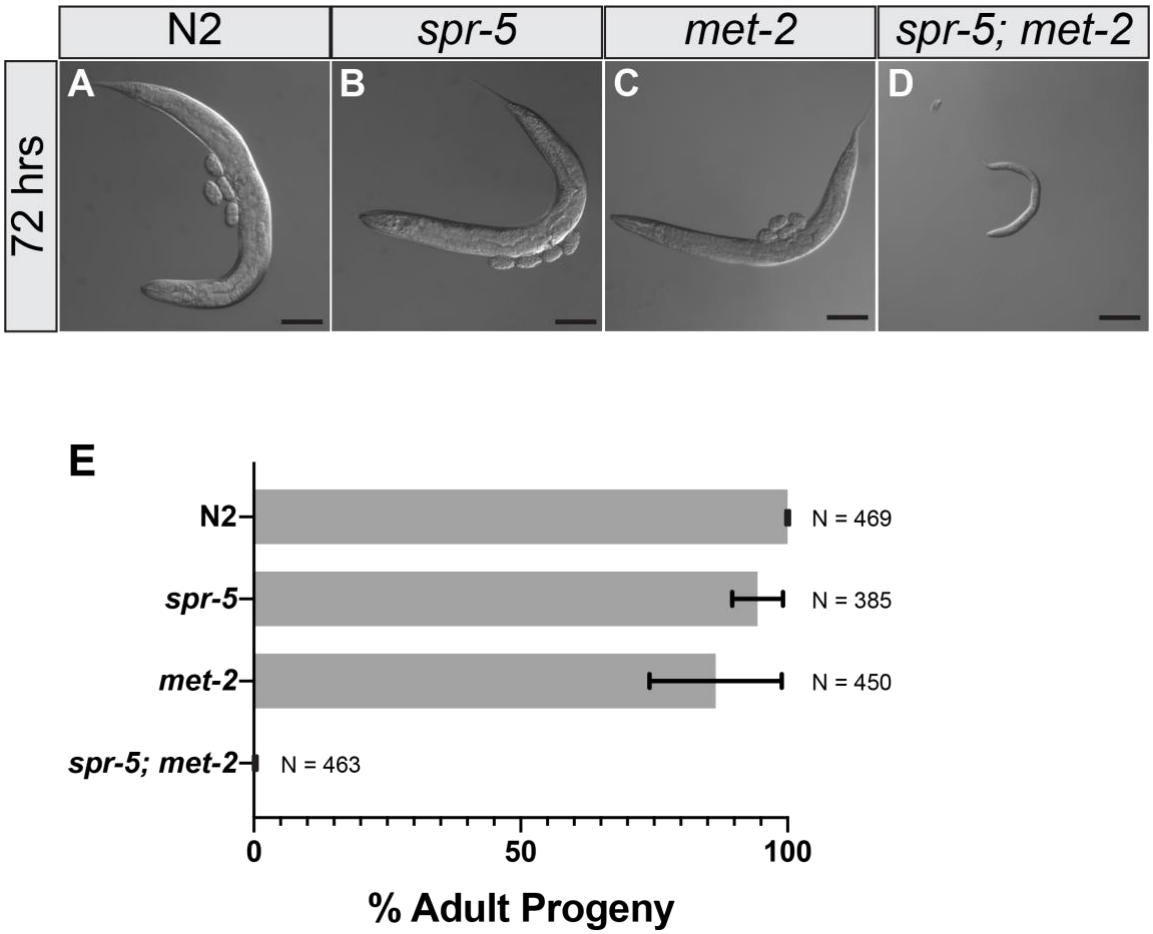

Figure 2. MES-4 germline genes are ectopically expressed in *spr-5; met-2* mutant soma. Overlap between MES-4 germline genes and genes up-regulated (A) and down-regulated (B) in *spr-5; met-2* L1 progeny. Significant over-enrichment in A was determined by the hypergeometric test (*p-value < 6.44e-20). (C) Heatmap of log2 fold change (FC) of 176 MES-4 germline genes in *spr-5, met-2* and *spr-5; met-2* mutants compared to N2. (D) Heatmap of log2FC of 176 MES-4 germline genes for the repeat *spr-5; met-2* RNA-seq experiment, with three additional biological replicates of *spr-5; met-2** mutants compared to N2 (see methods). Log2FC values are represented in a yellow to blue gradient and range from -2 to 5. Yellow represents genes with negative log2FC values and blue represents genes with positive log2FC values compared to N2. The remaining 21 MES-4 germline genes were not included because they do not have an expression value in one or more of the data sets (*spr-5*, *met-2,* or *spr-5; met-2*).

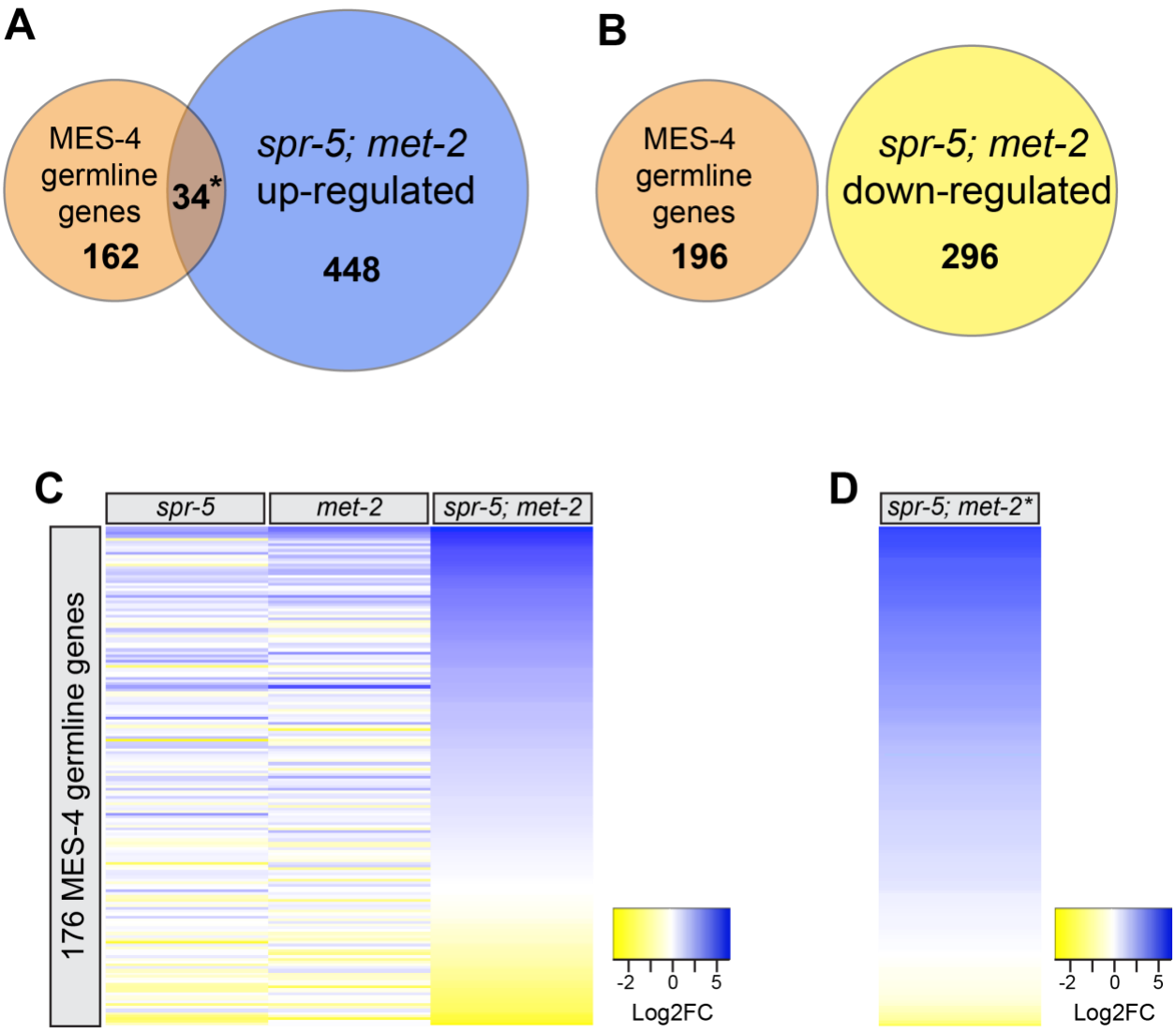

Figure 3. *spr-5; met-2* L1 progeny ectopically express MES-4 germline genes in multiple somatic tissues. 40x smFISH images of *htp-1* (A, C, D, F) and *cpb-1* (G, I, J, L) endogenous mRNAs in N2 (A-C, G-I) and *spr-5; met-2* (D-F, J-L) L1 progeny. DAPI was used as a nuclear marker (B, C, E, F, H, I, K, L). Insets are high magnification images of the germ cells, Z2 and Z3, in N2 L1 progeny. Arrows (J, L) denote ectopic *cpb-1* mRNA foci in somatic cells. Scale bar 40µm.

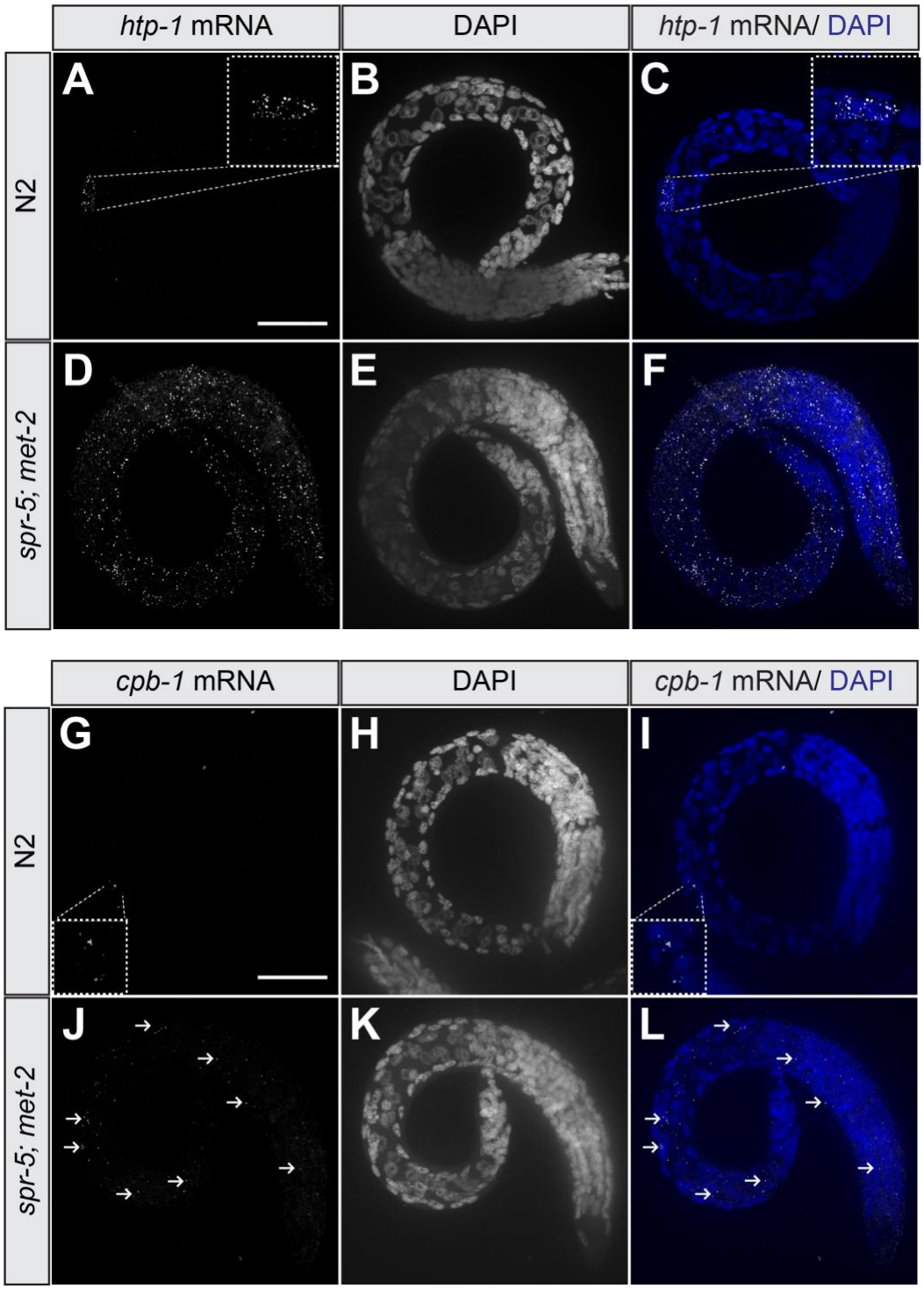

Figure 4. MES-4 germline genes display ectopic H3K36me3 in *spr-5; met-2* L1 progeny. Heatmap of H3K36me3 ChIP-seq reads normalized to reads per kilobase million (RPKM) over the gene bodies of 196 MES-4 germline genes in wild-type (N2) (A) versus *spr-5; met-2* (B) L1 progeny (second replicate in Figure S5). Gene bodies were pseudoscaled to 1kb with 500bp borders separated by orange bars that represent the transcriptional start site (TSS) and transcriptional end site (TES). Integrative Genome Viewer (IGV) image of H3K36me3 ChIP-seq reads normalized to RPKM at MES-4 germline genes (C-F, J-M) and control genes (G-I, N-P) in N2 (C-I) versus *spr-5; met-2* (J-P) L1 progeny. RPKM IGV windows were scaled between 0 and 202 RPKM for all genes.

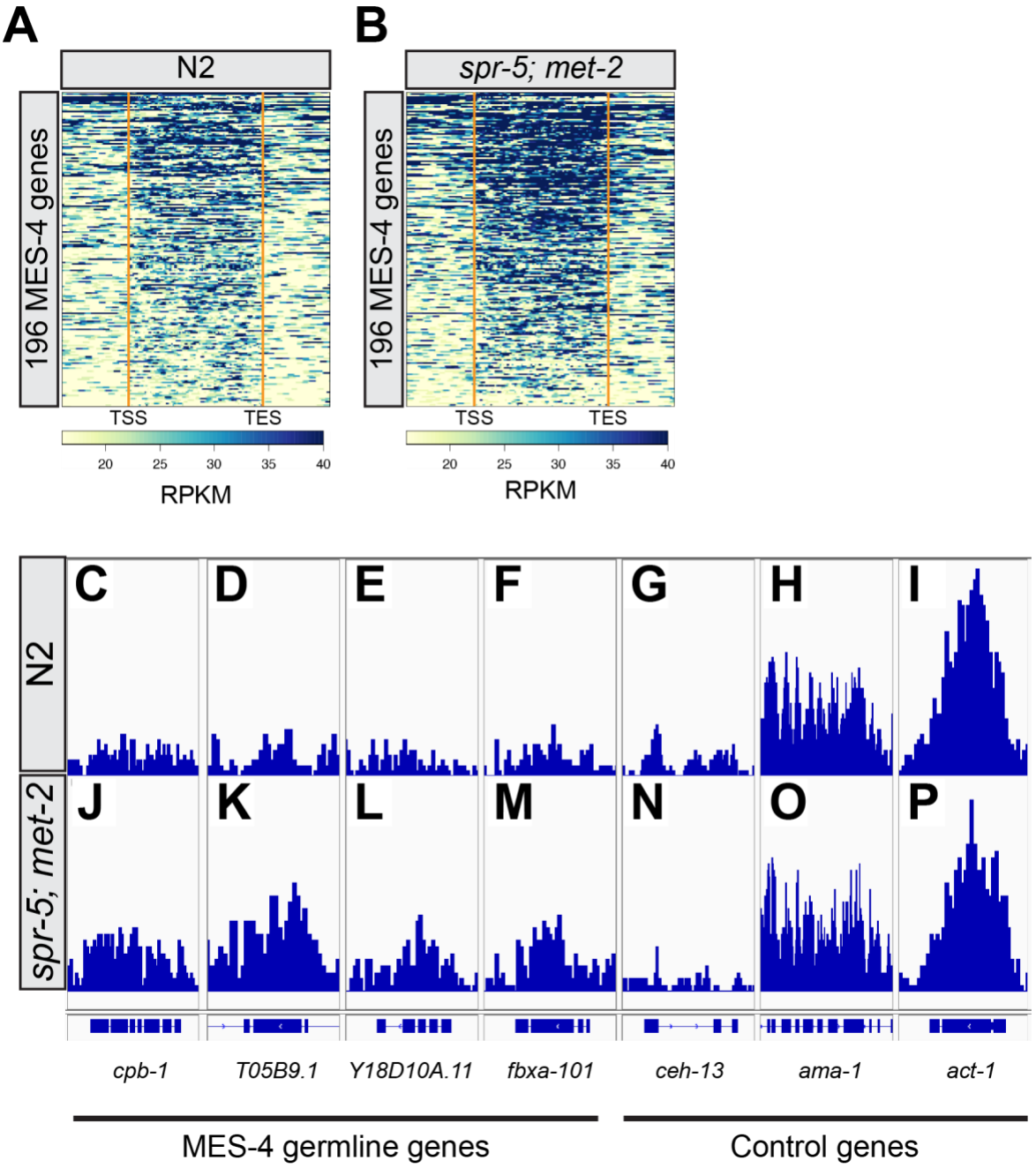

Figure 5. Knocking down MES-4 rescues ectopic expression of MES-4 germline genes in *spr-5; met-2* L1 progeny. Quantitative RT-PCR showing the relative units of expression for nine MES-4 germline genes (*cpb-1, csr-1*, *fbxa-101*, *htp*-1, *T05B9.1*, *Y18D10A.11*, *ftr-1*, *rmh-1*, *K12D12.5*) in L1 progeny of *spr-5; met-2* hermaphrodites fed either control L4440 RNAi (grey bars) or *mes-4* RNAi (black bars) versus N2 fed control L4440 RNAi (white bars). Relative units of expression from two biological replicates (R1 and R2) were calculated for each gene by averaging triplicate RT_PCR reactions and normalizing to a control gene, *ama-1*. Error bars represent the standard error of the mean (SEM) for triplicate RT_PCR reactions. For all nine genes, *mes-4* RNAi significantly reduced the relative expression of *spr-5; met-2* compared to *spr-5; met-2* fed L4440 control RNAi (unpaired t-test, p-value <0.001).

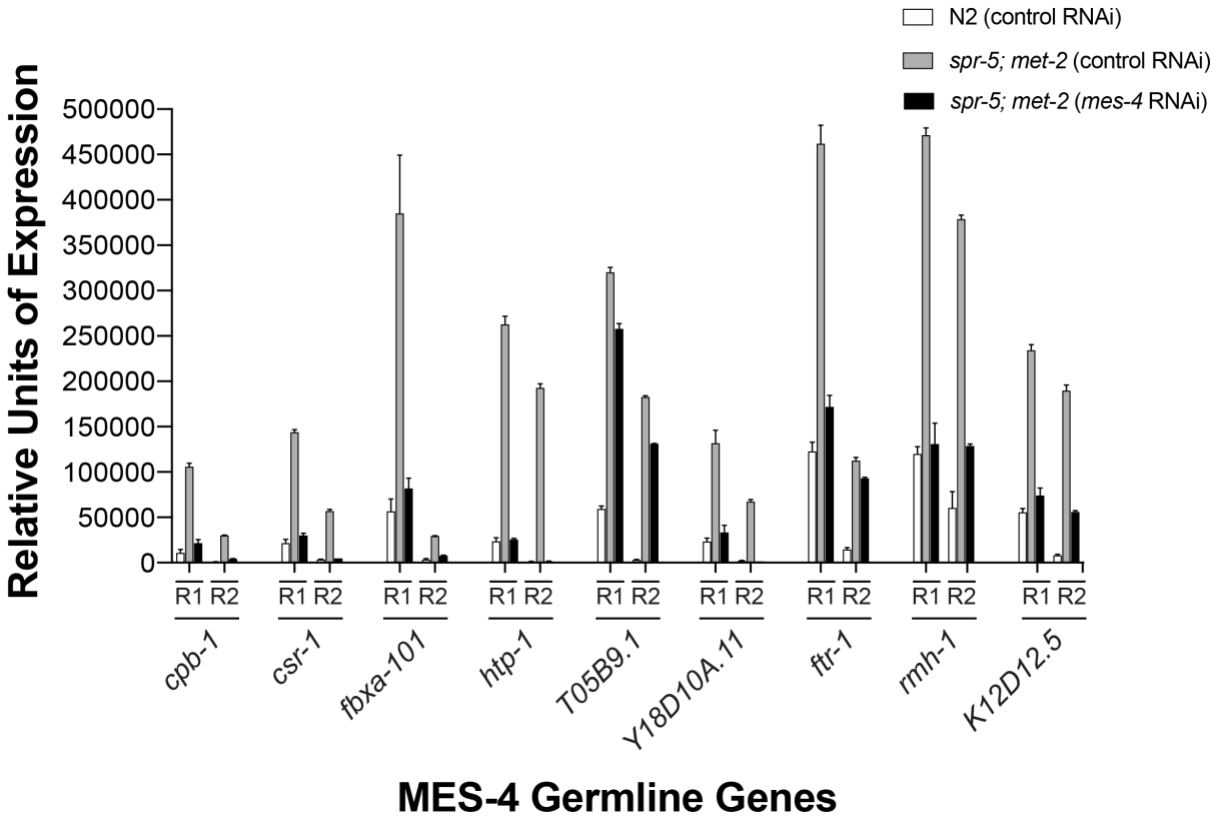

Figure 6. Knocking down MES-4 rescues developmental delay in *spr-5; met-2* progeny. DIC images of N2 (A-D) or *spr-5; met-2* (E-H) progeny from hermaphrodite parents treated with control (L4440 vector only) RNAi (A, E), *mes-4* RNAi (B, F), *met-1*RNAi (C, G), or *set-2* RNAi (D, H) 72 hours post synchronized lay. Scale bar: 100µm. (I) Quantification of the number of progeny (represented as % Adult Progeny) from A-H that made it to adults by 72 hours. Error bars represent the standard deviation of the mean from two or three experiments. N represents the total number of progeny from 30-40 hermaphrodites scored across independent experiments. (unpaired t-test, **** represent a p-value <0.0001).

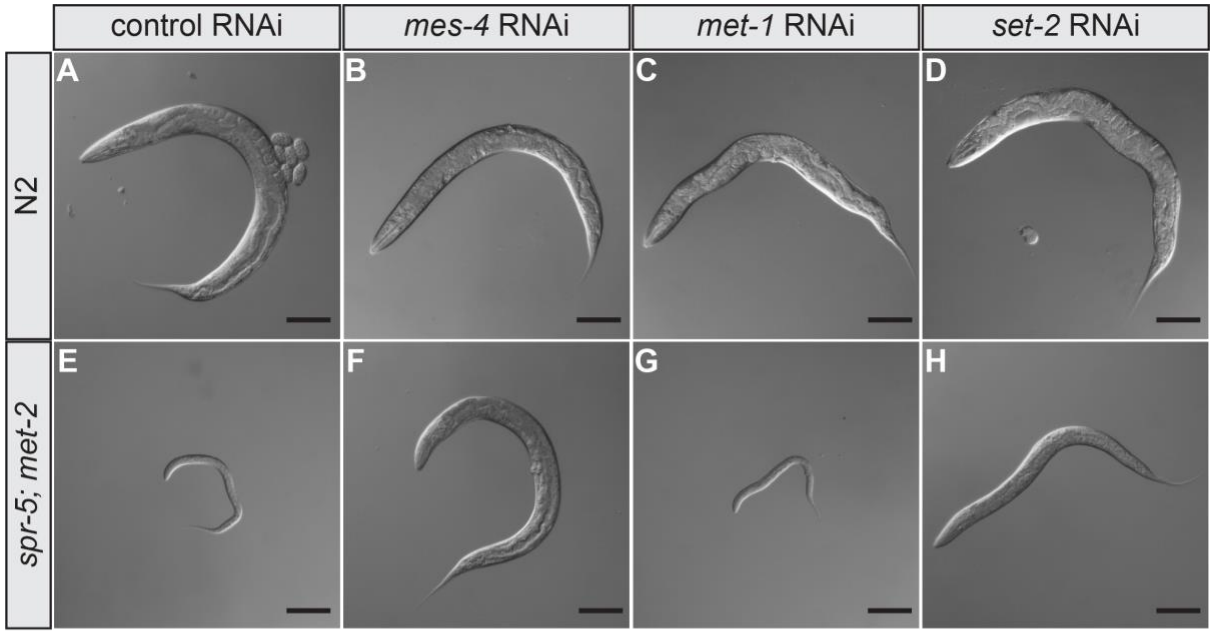

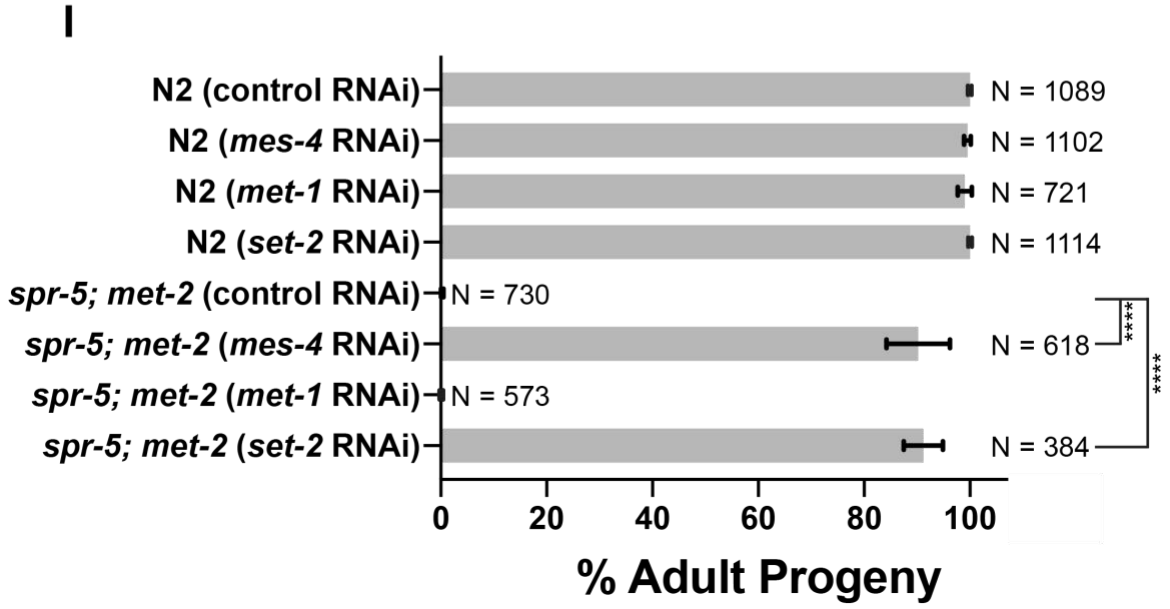

Figure 7. *let-858* transgene silencing in the soma of *spr-5; met-2* mutants. 40x differential contrasting interference (DIC) (A, C, E, G, and I) and immunofluorescent (B, D, F, H, and J) images of N2 (A-D) and *spr-5; met-2* (E-J) L2 progeny. Arrows denote faint expression of LET-858::GFP. Scale bar: 50 μm. Scale bar is the same for all panels. Percentage of animals where the expression level of LET-858::GFP was scored as either bright expressing (bright green, representative shown in panel B and F), faint expressing (dark green, representative shown in panel D and H), or not expressing (black, representative shown in panel J) in N2 (N=132) versus *spr-5; met-2* (N=87) progeny (K). The quantification represents the percentages of LET-858::GFP expressing progeny from two independent experiments. To control for the segregation of the *let-858* transgene, progeny scored as "off" were normalized for the presence of the *let-858* transgene in animals as detected by PCR (see methods).

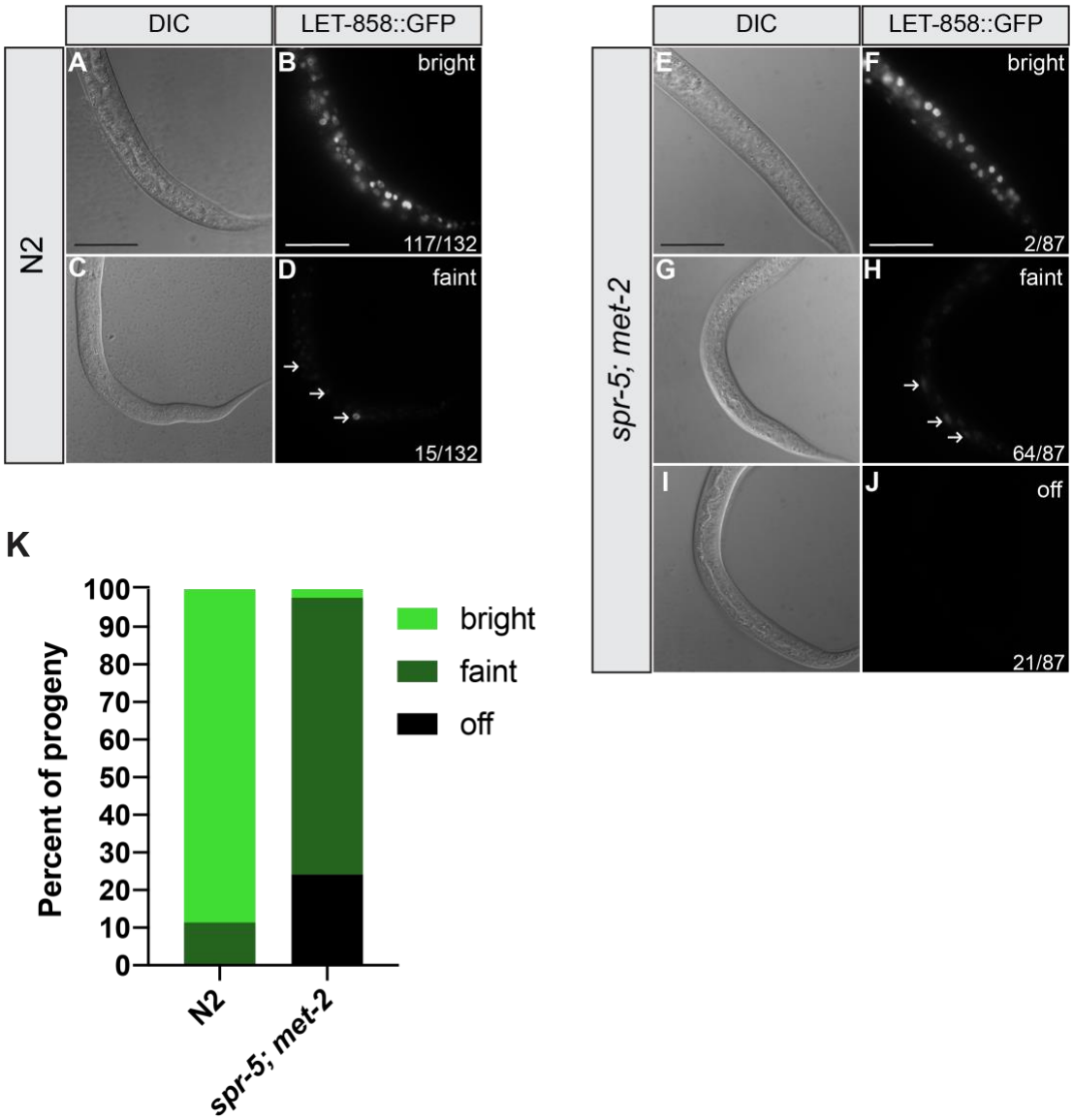

Figure 8: A model for how maternal reprogramming of inherited histone methylation helps to specify germline versus soma. During development, SET-2 and MET-1 add transcriptionally coupled H3K4me1/2 and H3K36me2/3 to germline expressed genes in the parental germline, respectively. (A) At fertilization, these germline expressed genes undergo maternal epigenetic reprogramming (establishment phase) by SPR-5 and MET-2 to remove H3K4me1/2 and add H3K9me1/2. In the germline blastomeres of the embryo, PIE-1 prevents global transcription by inhibiting POL-II. In the absence of transcription, MES-4 maintains H3K36me2/3 at MES-4 germline genes that have acquired transcriptionally coupled H3K36me2/3 in the previous germline. This enables these genes to avoid being repressed by maternal *spr-5; met-2* reprogramming and ensures that these genes remain bookmarked for re-expression once the germline begins to proliferate later in development. In addition, multiple systems, such as LIN-15B and LIN-35, as well as MEP-1 and LET-418, function in somatic tissues to further antagonize H3K36 bookmarking by MES-4 (maintenance phase). (B) Without SPR-5 and MET-2 maternal reprogramming, H3K4me1/2 is inappropriately inherited in somatic tissues, allowing MES-4 to ectopically add H3K36me2/3 at these germline genes. This leads to ectopic expression of MES-4 germline genes in somatic tissues and a severe developmental delay. Orange circles represent somatic cells, Grey circles outlined in blue dashed-lines represent germ cells, and orange circles outlined in dashed-blue lines depict somatic cells that ectopically express MES-4 germline genes. P-lineage, germline blastomeres, are indicated by the letter P, and the primordial germline cells are indicated by Z2 and Z3.

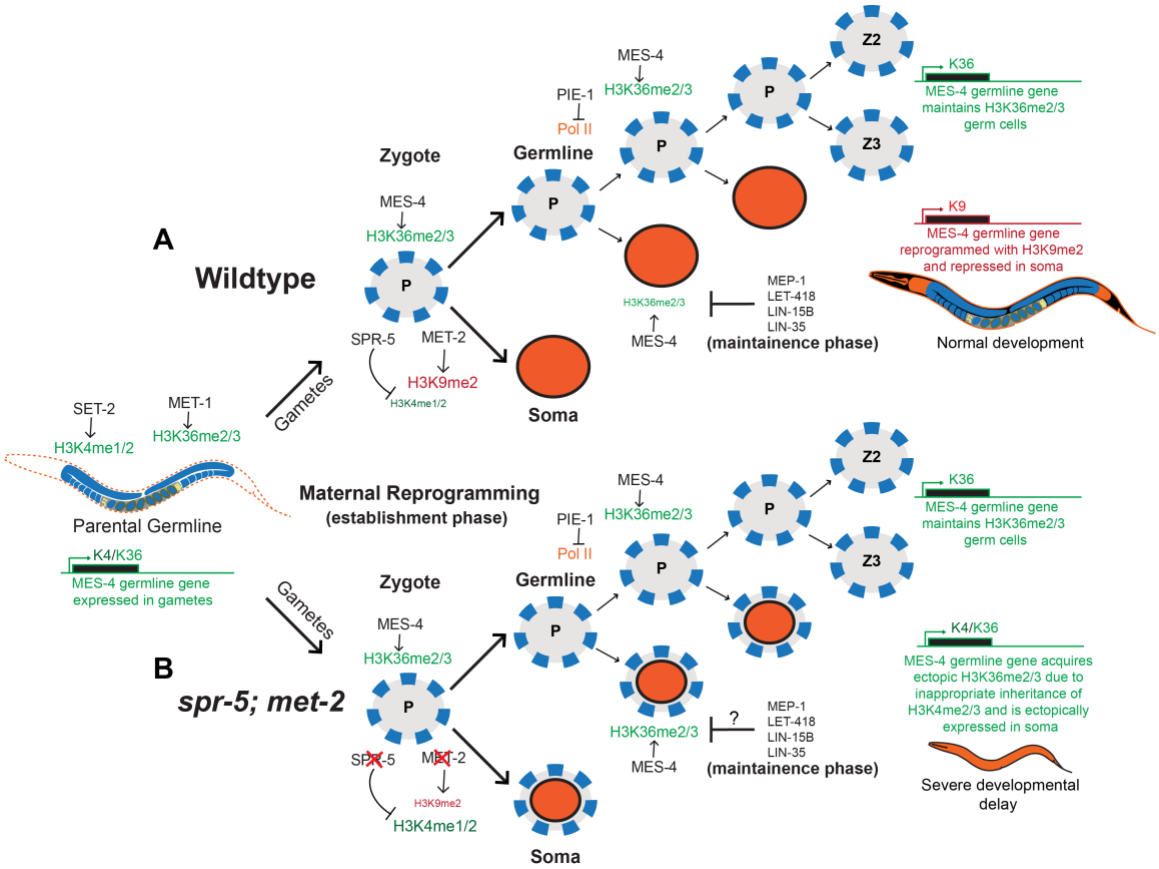

Figure 1 - supplement figure 1. *spr-5; met-2* mutants display severe developmental delay and protruding vulva. 40x DIC images of N2 (A), *spr-5* (B), *met-2* (C), and *spr-5; met-2* (D) progeny at 72 hours post synchronized lay. DIC image in (D) was magnified an additional 4x. 40x DIC images of two examples of *spr-5; met-2* adult progeny (E, F) at seven days post synchronized lay. Dashed-line (D) outlines germline and asterisks (E, F) denote protruding vulva. Scale bar: 100µm. (G) Quantification of *spr-5; met-2* progeny that reached the adult stage by seven days post synchronized lay, along with quantification of protruding vulva (Pvl) in these animals that reached the adult stage. The 876 progeny scored came from a total of 25 hermaphrodites across two independent experiments.

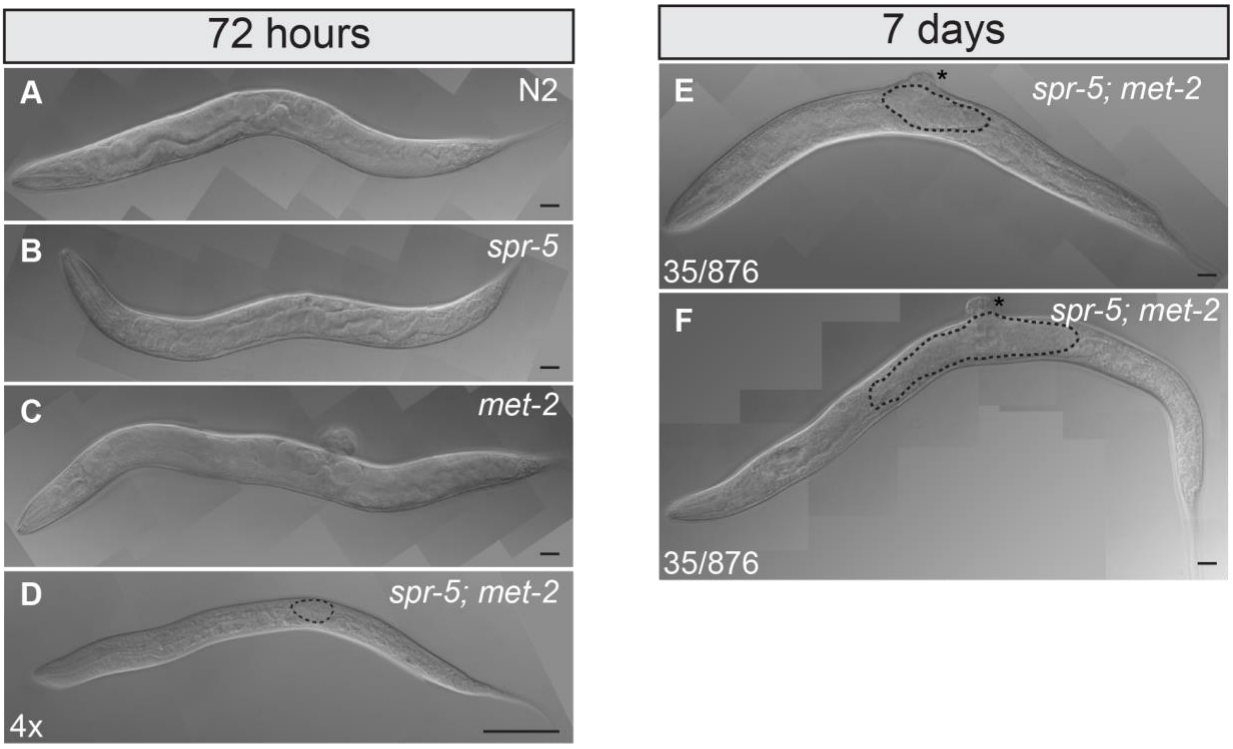

G

Total # of progeny scored	Total # of adult progeny	Percent of adult progeny	Total # of adult progeny with Pvl	Percent of adult progeny with Pvl
876	35	3.9%	31	88.5%

Figure 2 - supplement figure 1. Differential gene expression in *spr-5, met-2, and spr-5; met-2* progeny *compared* to N2 progeny. (A) Table summary of differentially expressed genes in *spr-5, met-2, and spr-5; met-2* L1 progeny from DESEQ2 analysis (significance cut-off of p-value < 0.05). (B) Overlap of differentially expressed genes between *spr-5, met-2, and spr-5; met-2* L1 progeny. Gene Ontology analysis showing Biological Processes (C) and Cellular Components (D) amongst genes that were up-regulated (red) and down-regulated (green) in *spr-5; met-2* L1 progeny compared to N2. Combined Score was computed to determine gene set enrichment (Chen et al., 2013) (see source data file 1 for gene ontology R scripts).

A

Genotype	Total # of differentially expressed genes	Up-regulated	Down-regulated
spr-5	343	259	84
met-2	413	262	151
spr-5; met-2	778	482	296

B

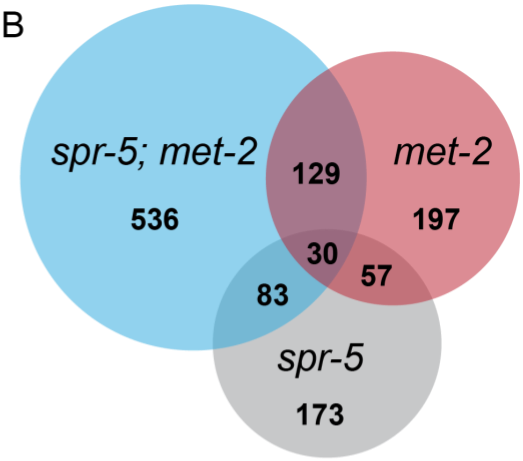

C

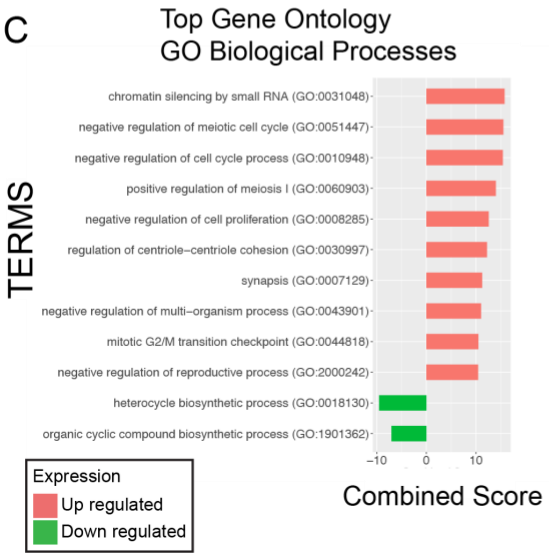

D

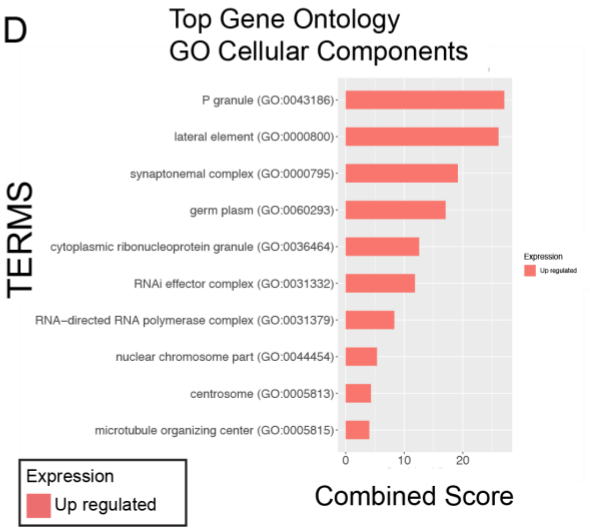

Figure 2 - supplement figure 2. Differential expression and replicate comparison of RNAseq experiments performed on N2, *spr-5*; *met-2*, and *spr-5; met-2* L1 progeny. Volcano plot of log2 fold changes in gene expression (x-axis) by statistical significance (-Log10 P-value; y-axis) in *spr-5* (A), *met-2* (B), and *spr-5; met-2* (C) L1 Progeny compared to N2 (see source data file 2 for volcano plot R scripts). Heatmap of differentially expressed RNA-seq transcripts between N2 and *spr-5* (D), *met-2* (E), and *spr-5; met-2* (F). Data was scaled and hierarchical clustering was performed using the complete linkage algorithm. Distance was measured by calculating pairwise distance. Higher (red) and lower (green) expression is reported as a z-score. (see source data file 3 for heatmap R scripts).

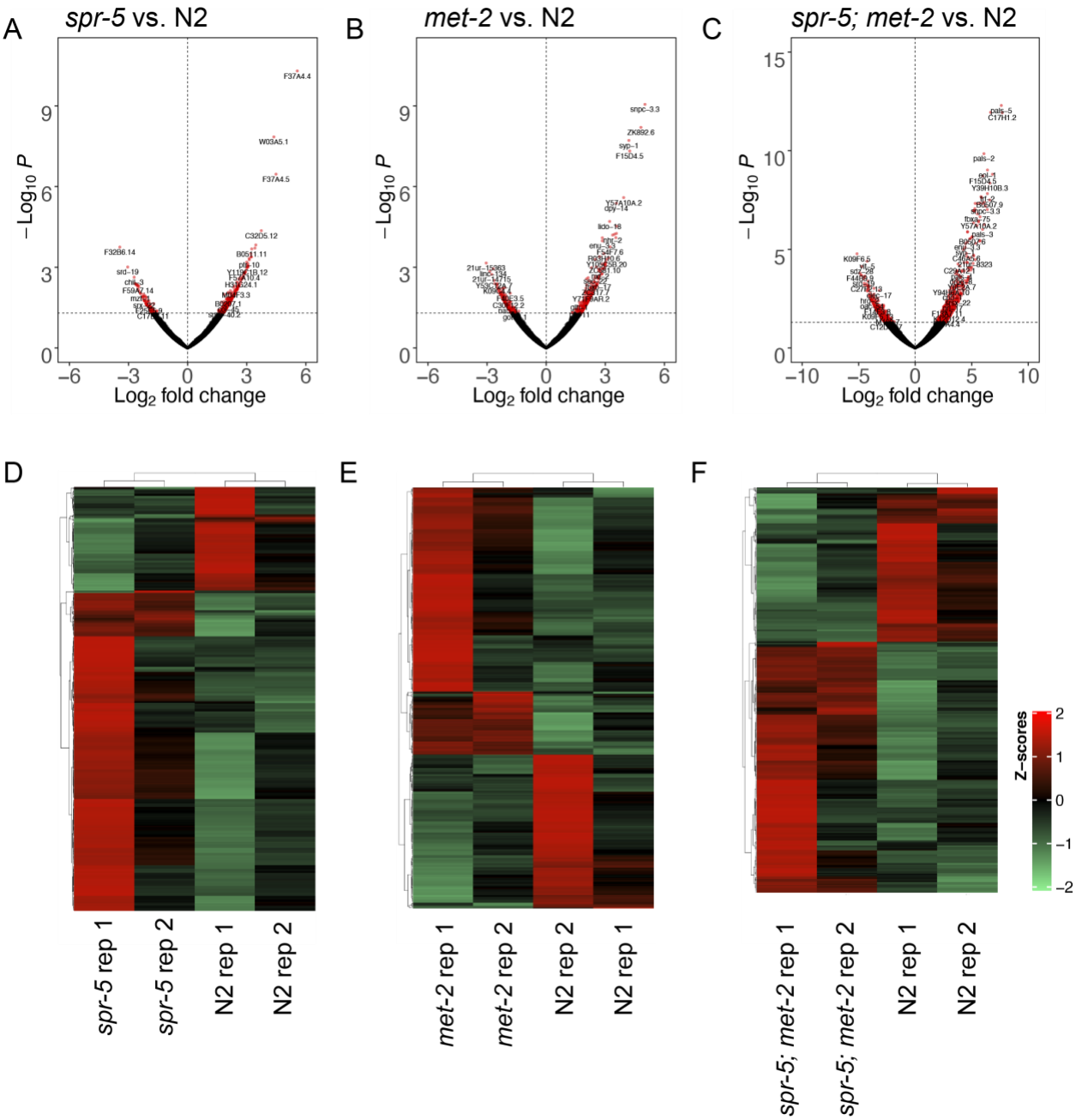

Figure 2-supplemental figure 3. MES-4 germline genes are ectopically expressed in *spr-5; met-2* mutant soma in the RNAseq repeat experiment. Overlap between MES-4 germline genes and genes up-regulated (A) and down-regulated (B) in *spr-5; met-2* L1 progeny. Significant over-enrichment in A was determined by the hypergeometric test (*P-value < 1.20E-54). (C) Heatmap of log2 fold change (FC) of 176 MES-4 germline genes in *spr-5; met-2* mutants compared to N2 (2 replicates, low-input, see methods) vs. repeat of *spr-5; met-2** mutants compared to N2 (*3 replicates, standard Poly-A selection, see methods). Log2FC values are represented in a yellow to blue gradient and range from -2 to 5 and were sorted by the average log2FC in *spr-5; met-2* and *spr-5; met-2** progeny. Yellow represents genes with negative log2FC values and blue represents genes with positive log2FC values compared to N2. The remaining 21 MES-4 germline genes were not included because they do not have an expression value in one or more of the data sets (*spr-5; met-2* or *spr-5; met-2**).

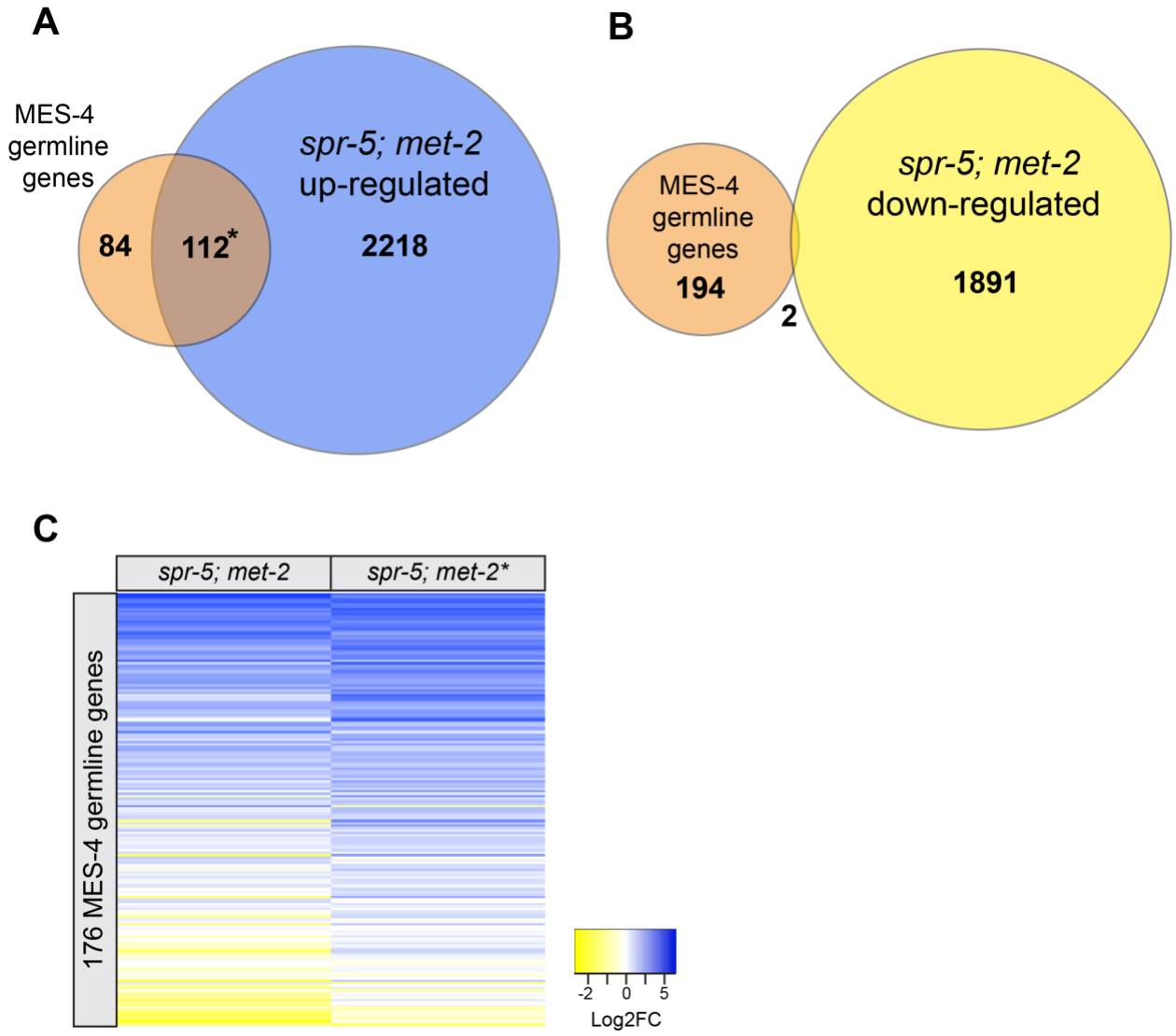

Figure 3 - supplement figure 1. smFISH control experiments. smFISH images of *ama-1* mRNA (A, C, D, F) and a no probe control (G, I, J, L) in N2 (A-C, G-I) and *spr-5; met-2* (D-F, J-L) L1 progeny. DAPI was used as a nuclear marker (B, C, E, F, H, I, K, L). Scale bar 40µm.

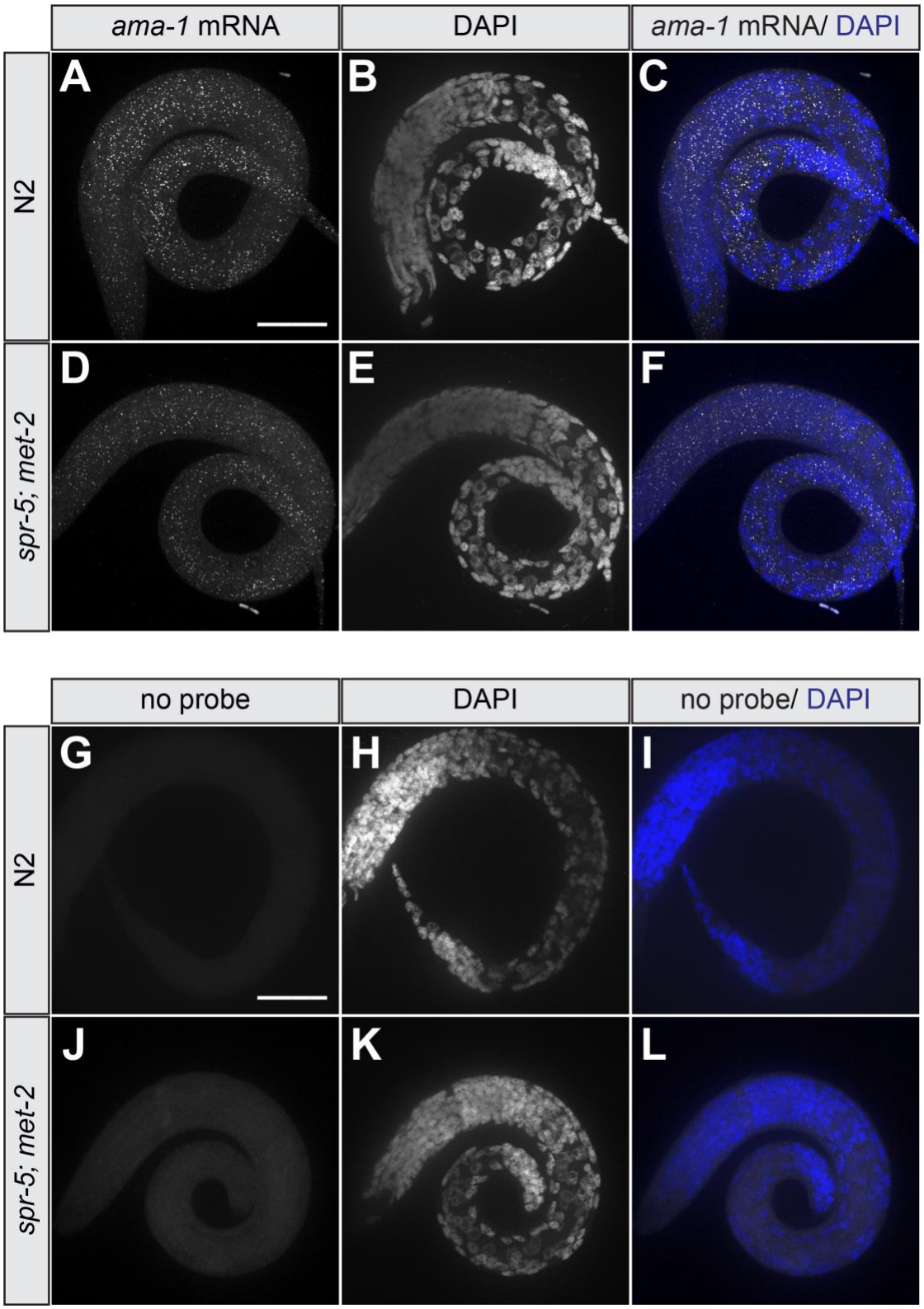

Figure 4 - supplement figure 1. Replicate comparison of H3K36me3 ChIP-seq analysis in *spr-5; met-2* L1 progeny. Heatmap of H3K36me3 ChIP-seq reads from a second replicate (1st replicate in Figure 4) normalized to reads per kilobase million (RPKM) over the gene bodies of 196 MES-4 germline genes in wild-type (N2) (A) versus *spr-5; met-2* (B) L1 progeny. Gene bodies were pseudoscaled to 1kb with 500bp borders separated by orange bars that represent the transcriptional start site (TSS) and transcriptional end site (TES). Integrative Genome Viewer (IGV) image of H3K36me3 ChIP-seq reads from replicate 2 normalized to RPKM at MES-4 germline genes (C-F, J-M) versus control genes (G-I, N-P) in N2 (C-I) and *spr-5; met-2* (J-P) L1 progeny. RPKM IGV windows were scaled between 0 and 107 RPKM for all genes. Venn-diagram displaying the overlap of H3K36me3 ChIP-seq called broad peaks for N2 (Q) and *spr-5; met-2* (R) replicates.

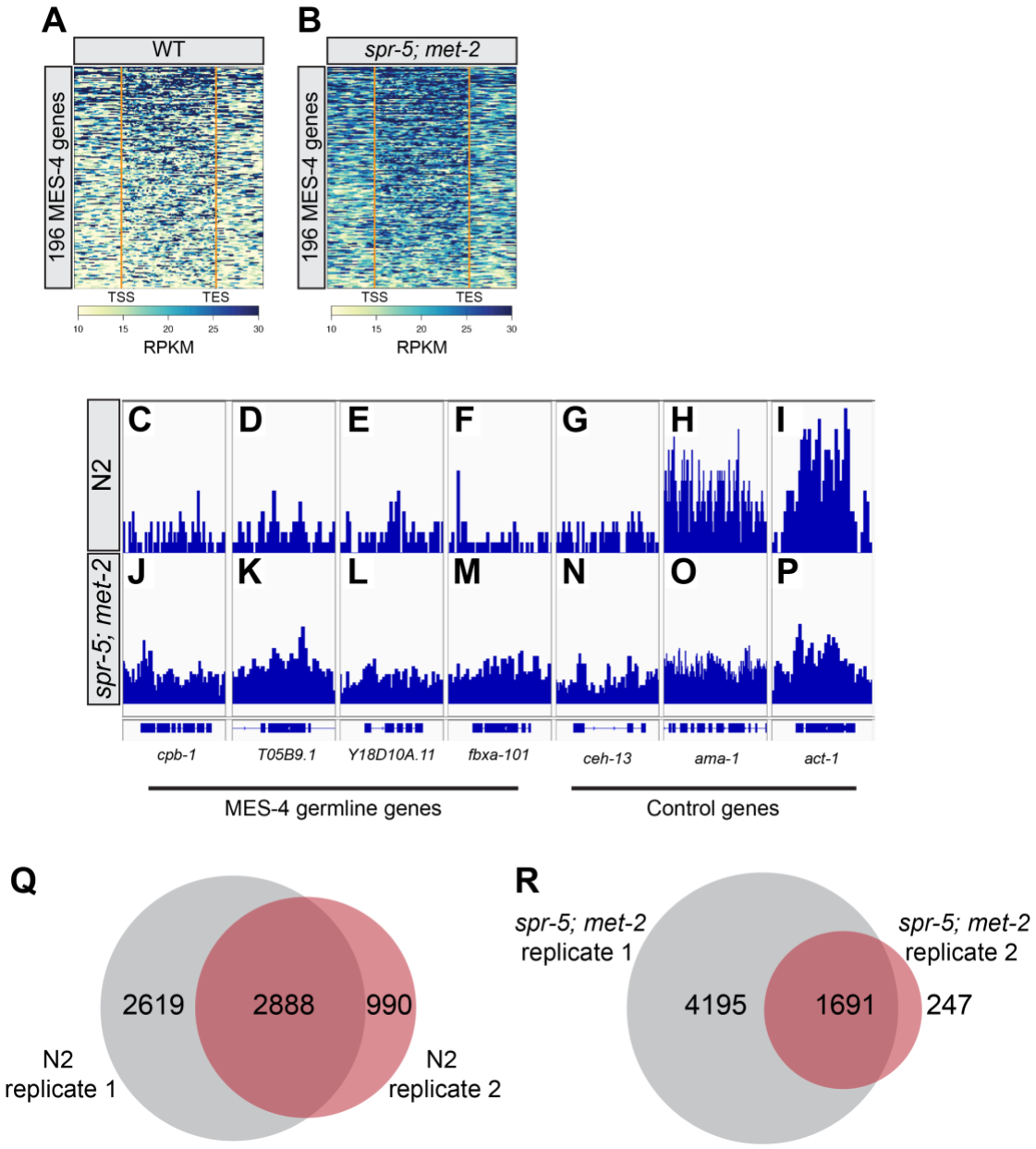

Figure 4 - supplement figure 2. MES-4 germline genes display H3K9me2 at their promoters. Heatmap of H3K9me2 promoter peaks in N2 L1 progeny at all 196 MES-4 germline genes (A), and at the 34 MES-4 germline genes that were ectopically expressed in the soma of *spr-5; met-2* progeny (B). ChIP-seq reads were scaled to genome wide coverage for H3K9me2 (15 million reads). The transcriptional start site (TSS) is denoted by an orange bar with 500bp flanking regions upstream and downstream of the TSS. Integrative Genome Viewer (IGV) image of ChIP-seq reads from N2 L1 progeny scaled to genome wide coverage for H3K9me2 (15 million reads) over the promoters of MES-4 germline genes that were ectopically expressed in the soma of *spr-5; met-2* progeny (C-F) and control genes (G-I). IGV windows were scaled between 0 and 255 RPKM. Asterisks (*) denotes H3K9me2 promoter peaks at MES-4 germline genes.

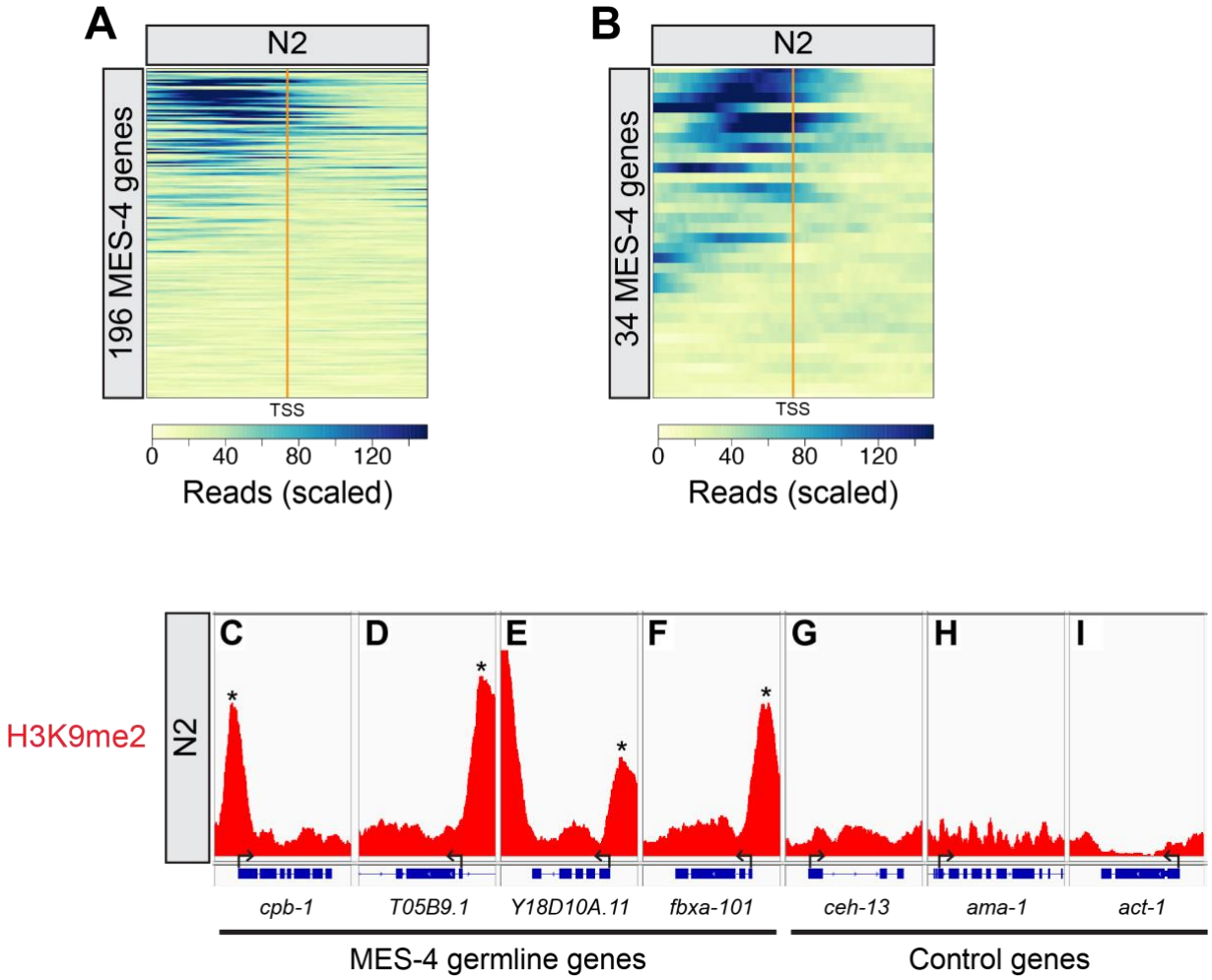

Supplementary file 1. **Raw scores for developmental delay in N2, *spr-5*, *met-2*, and *spr-5; met-2* progeny.** Progeny were scored 72 hours after a synchronized lay as developing to the L1, L2, L3, L4, or young adult (YA) stage (Figure 1A-E). N= the total number of progeny from a total of 20-25 hermaphrodites scored over three experiments.

Supplementary file 2. **Differentially expressed transcripts in *spr-5*, *met-2*, and *spr-5; met-2* progeny**. List of differentially expressed transcripts in *spr-5*, *met-2*, *spr-5; met-2* (Wald test, P-value<0.05), and the repeat RNA-seq experiment with three additional *spr-5; met-2* replicates (Wald test, P-adj<0.05) L1 progeny compared to N2 progeny from DESEQ2 analysis (Figure 2-supplement figure 2A-D).

Supplementary file 3. **176 MES-4 germline gene log2(FC) values used to generate heatmap.** The log2(FC) values of the 176 MES-4 germline genes from the DESEQ2 analysis performed on *spr-5, met-2, spr-5; met-2*, and the repeat RNA-seq experiment of *spr-5; met-2* (*) L1 progeny compared to N2 progeny. log2(FC) values were sorted from highest to lowest based on the differential expression of genes in *spr-5; met-2* progeny compared to N2 (Figure 2C-D).

Supplementary file 4. smFISH probe sequences. List of smFISH probe sequences for *htp-1* and *cpb-1* used in smFISH experiments (Figure 3).

Supplementary file 5. Primer sequences used for genotyping and RT-PCR. List of genotyping primers and RT-PCR primers (Figure 5).

Supplementary file 6. Raw values from Quantitative RT-PCR analysis. Raw SQ means and standard deviations for RT-PCR experiments (Figure 5).

Source data file 1. R scripts for gene ontology (Figure 2-supplement figure 1C-D)

Source data file 2. R scripts for volcano plots (Figure 2-supplement figure 2A-C)

Source data file 3. R scripts for heatmaps (Figure 2-supplement figure 2D-F)